

Phosphoribosyl modification of poly-ubiquitin chains at the *Legionella*-containing vacuole prohibiting autophagy adaptor recognition

Received: 27 August 2023

Accepted: 4 June 2024

Published online: 30 August 2024

 Check for updatesMin Wan^{1,2,4}, Marena E. Minelli^{1,2,4}, Qiuye Zhao¹, Shannon Marshall¹, Haiyuan Yu^{1,3}, Marcus Smolka^{1,2} & Yuxin Mao^{1,2} ✉

Ubiquitination is a posttranslational modification in eukaryotes that plays a significant role in the infection of intracellular microbial pathogens, such as *Legionella pneumophila*. While the *Legionella*-containing vacuole (LCV) is coated with ubiquitin (Ub), it avoids recognition by autophagy adaptors. Here, we report that the Sdc and Sde families of effectors work together to build ubiquitinated species around the LCV. The Sdc effectors catalyze canonical polyubiquitination directly on host targets or on phosphoribosyl-Ub conjugated to host targets by Sde. Remarkably, Ub moieties within poly-Ub chains are either modified with a phosphoribosyl group by PDE domain-containing effectors or covalently attached to other host substrates via Sde-mediated phosphoribosyl-ubiquitination. Furthermore, these modifications prevent the recognition by Ub adaptors and therefore exclude host autophagy adaptors from the LCV. In this work, we shed light on the nature of the poly-ubiquitinated species present at the surface of the LCV and provide a molecular mechanism for the avoidance of autophagy adaptors by the Ub-decorated LCV.

Autophagy is a major degradation pathway that is activated in various stress conditions such as starvation, organelle damage, and pathogen invasion^{1,2}. Autophagy is initiated by the activation of the ULK1 serine/threonine kinase, which assembles a complex with FIP200, ATG13, and ATG101 at the phagophore formation site³. Activated ULK1 promotes the recruitment of class III PI3K complex to the phagophore, where PI(3)P is generated to facilitate autophagosome nucleation⁴. The expansion and maturation of autophagosomes are facilitated by two ubiquitin-like conjugation systems, through which, the ubiquitin-like LC3 is conjugated to phosphatidylethanolamine (PE) at both the inner and outer membranes of the phagosome^{5,6}. Mature phagosomes need to fuse with lysosomes to achieve autophagic degradation. Although

autophagy was originally discovered as a nonselective bulk degradation process in response to starvation⁷, selective autophagy that targets specific substrates for degradation was later characterized by a myriad of studies⁸. Many types of selective autophagy involve the ubiquitination of cargoes, which are then recognized by ubiquitin-binding autophagy adaptor proteins (autophagy receptors). Specific autophagy adaptors, such as p62/SQSTM1, NDP52, and OPTN, contain ubiquitin-binding domains and conserved LC3-interacting regions (LIR) and recruit ubiquitinated cargoes to the LC3-positive autophagy compartment⁹.

Xenophagy, one type of ubiquitin-dependent selective autophagy, is a key mechanism for the host to defend against the

¹Weill Institute for Cell and Molecular Biology, Cornell University, Ithaca, NY, USA. ²Department of Molecular Biology and Genetics, Cornell University, Ithaca, NY, USA. ³Department of Computational Biology, Cornell University, Ithaca, NY, USA. ⁴These authors contributed equally: Min Wan, Marena E. Minelli.

✉ e-mail: ym253@cornell.edu

invasion of intracellular pathogens, such as *Shigella flexneri*, *Listeria monocytogenes*, and *Salmonella enterica*^{10,11}. During infection, Ub can be attached to pathogens or pathogen-containing vacuoles by ubiquitin E3 ligases to generate a “Ub-coat” surrounding the pathogen. The Ub-coat serves as a signaling platform to recruit autophagy adaptors and thus drive the sorting of the cargo into the autophagic vacuole for degradation. Among the autophagy adaptors, p62 is the best-studied molecule involved in the xenophagy of many kinds of pathogens⁸.

Legionella pneumophila is an opportunistic intracellular bacterial pathogen that causes a severe form of pneumonia called Legionnaires’ disease^{12,13}. After *L. pneumophila* is phagocytosed in host cells, this bacterium secretes over 350 effector proteins into the host through the Dot/Icm, a type IV secretion system (T4SS)^{14,15}. These bacterial effector proteins hijack various host cellular pathways to create an optimal niche, the *Legionella*-containing vacuole (LCV), for robust bacterial intracellular growth¹⁶. Among these host cellular pathways, the ubiquitination pathway is a prime target of this intracellular pathogen. Ubiquitination is one of the most essential eukaryotic posttranslational modifications (PTMs) that regulates a plethora of physiological processes, including protein homeostasis¹⁷, cell signaling¹⁸, and membrane trafficking^{19,20}. It has been shown that the surface of the LCV is positive for Ub signals as early as 1 hour post infection (hpi) and remains positive throughout the infection²¹. Later studies revealed that the Ub-coat around the LCV contains both K48 and K63-linked Ub chains²². The *Legionella* Sdc family of effectors (SidC and SdcA), which have a unique HECT-type Ub E3 ligase-like domain, have been shown at least partially to be responsible for the accumulation of ubiquitinated species around the LCV^{23,24}. Besides the Sdc effectors that catalyze canonical ubiquitination, the Sde family of effectors (SdeE, SdeA, SdeB, and SdeC) also play a role in the accumulation of Ub signals at the LCV²⁵. Sde effectors are a group of novel Ub ligases that act independently of ATP, Mg²⁺, or E1 and E2 enzymes^{26–28}. The Sde family enzymes first catalyze ADP-ribosylation on Ub to generate mono-ADP-ribosyl Ub (ADPR-Ub) via the mono-ADP-ribosyl transferase (mART) domain. Next, the intermediate product, ADPR-Ub, can be either conjugated to serine or tyrosine residues on substrates (phosphoribosyl- or PR-ubiquitination) or hydrolyzed to phosphoribosyl-Ub (PR-Ub) via their phosphodiesterase (PDE) domain^{29–35}.

Surprisingly, although the LCV is enriched with ubiquitinated species, ubiquitin-binding autophagy adaptors are excluded from the LCV³⁶. Previous studies showed that *L. pneumophila* applies multiple strategies to avoid host autophagy. The *Legionella* effector RavZ irreversibly deconjugates lipidated LC3 on autophagosomal membranes and thus prevents autophagy-mediated degradation of the LCV³⁷. Another effector LpSPL hydrolyzes host sphingolipids and inhibits basal autophagy^{38,39}. Furthermore, the *Legionella* effector Lpg1137 was identified as a serine protease responsible for the cleavage of syntaxin 17 and hence blocks autophagy and BAX-induced apoptosis^{40,41}. These findings suggest that multiple mechanisms may exist for the bacterium to avoid clearance by autophagy.

In this study, we demonstrate the cross-talk between the Sdc and Sde families of effectors. We show that Sdc and Sde work together to build mixed poly-Ub chains on host substrates and both of these two families of effectors are required for the accumulation of ubiquitinated species around the LCV. Surprisingly, Sde proteins further modify poly-Ub chains by phosphoribosylation on residue Arg42 of Ub moieties or directly conjugate the poly-Ub chain to other host substrates via PR-ubiquitination. These modifications block the binding by the autophagy adaptor p62 to the Ub-enriched LCV and serves as an alternative mechanism to evade host autophagy.

Results

Both the Sdc and Sde effectors are required for the enrichment of ubiquitinated species at the LCV

Previous studies reported that shortly after *L. pneumophila* infection, ubiquitinated conjugates were accumulated at the bacterial phagosome^{21,22}. The Sdc enzymes, which function as HECT-type E3 ligases, were shown to be required for the enrichment of Ub signals at the LCV^{23,24}. Interestingly, the Sde proteins were also shown to influence Ub signals at the LCV²⁵. To elucidate the roles of these two distinct families of Ub ligases in LCV biogenesis, we analyzed the dynamics of Ub signals at the LCV during *L. pneumophila* infection. FcyRII-expressing HEK293T cells were challenged with the wild-type (WT) *L. pneumophila* Lp02 strain, ~81% of LCVs were stained positive for Ub at the early stage of infection (1–2 hpi), and then gradually decreased at later time points of infection (Fig. 1a, b). The accumulation of ubiquitinated species around the LCV was dependent on the Dot/Icm secretion system, as no Ub signals were detected in cells infected with the $\Delta dotA$ mutant strain. In agreement with previous results^{23,24}, the enrichment of Ub signals at the LCV was markedly reduced (~8%) in cells challenged with the Δsdc (*sidC* and *sdcA*) strain at 1 hpi. However, the percentage of Ub-positive LCVs recovered, albeit to a lesser extent compared to the WT strain, at later time points of infection (~19% at 2 hpi and ~25% at 6 hpi) (Fig. 1a, b). The Ub signals at the LCV were also substantially reduced in cells challenged with the Δsde (*sdeE*, *sdeA*, *sdeB*, and *sdeC*) strain with ~36% of LCVs positive for Ub at 1 hpi. In contrast to the Δsdc strain, the percentage of Ub-positive LCVs further dropped at later infection time points (as low as ~12% at 6 hpi) (Fig. 1a, b) suggesting Sde effectors are important in stabilizing ubiquitinated species at the LCV. Strikingly, the Ub signals were nearly completely abolished at the LCV in cells infected with the $\Delta sde/sdc$ strain (Fig. 1a, b). These observations suggest that both Sdc and Sde are the primary factors responsible for the enrichment of ubiquitinated species at the LCV.

Multiple host proteins are modified by both Sdc and Sde during *Legionella* infection

It has been shown that some host proteins, such as Rab1 and Rab10, are targeted by both Sdc and Sde families of effectors^{23,26,42}. We hypothesized that the accumulation of ubiquitinated species at the LCV is due to direct ubiquitination and PR-ubiquitination on the same host targets by Sdc and Sde, respectively. To test whether Sdc and Sde work together to modify the same host targets, we first analyzed the ubiquitination state of Rab1 in cells after *L. pneumophila* infection. HEK293T cells were transfected with plasmids expressing 3xFlag-Rab1 and FcyRII for 24 h and were challenged with WT or mutant *Legionella* strains for 1 h. Rab1 was then immunoprecipitated and analyzed by Western blot (Fig. 1c, d). Strong ubiquitinated Rab1 signals were detected in samples infected with WT *Legionella* strain but the signals were notably reduced in samples infected with either the Δsde or Δsdc strain. Furthermore, the ubiquitinated Rab1 signals were nearly abolished in the samples infected with the $\Delta sde/sdc$ strain. The Sdc and Sde-dependent ubiquitination/PR-ubiquitination of host targets was not limited to Rab1 as several other previously reported Sde substrates, Rab33B²⁶, the autophagosomal SNARE protein Stx17⁴³, and an ER membrane protein, LULL1⁴⁴ showed a similar Sdc and Sde-dependent ubiquitination during *Legionella* infection (Supplementary Fig. 1a–c). Our data suggests that multiple host proteins can be both ubiquitinated and PR-ubiquitinated by Sdc and Sde.

This observation was further supported by the treatment of immunoprecipitated substrates with a canonical DUB (the N-terminal deubiquitinase domain of SdeA)²⁵ and/or a PR-ubiquitination specific deubiquitinase (DupB)⁴⁴. Immunoprecipitated Rab1 was first prepared from cells infected with *Legionella* strains and was treated with deubiquitinases before Western blot analysis. The high molecular weight bands, corresponding to the poly-ubiquitinated Rab1, were

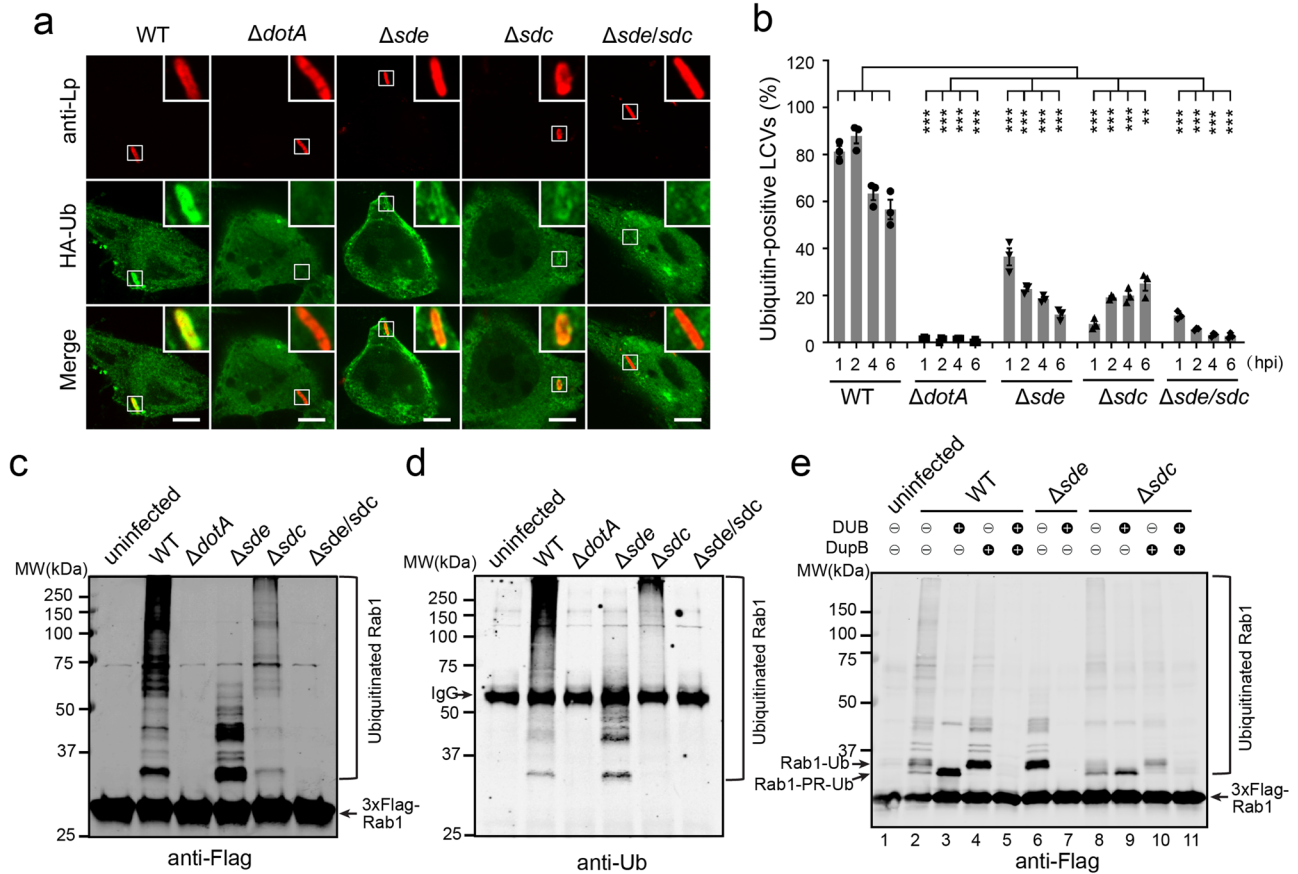


Fig. 1 | The *sde* and *sdc* families of effectors are required for the ubiquitination of host targets and the enrichment of ubiquitinated species at the LCV.

a Representative confocal images showing the Ub signals (green) at the LCV in HEK293T cells challenged with specified *Legionella* strains (red) at 1 hpi. Scale Bar: 5 μm. **b** Quantitative analysis of Ub-positive LCVs in cells infected with the indicated *Legionella* strains. Data were shown as means ± SEM of three independent experiments. At least 45 randomly selected LCVs were counted for each condition. Statistical comparisons between two groups were conducted using unpaired two-tailed Student's *t*-tests. The *P* values (1 h, 2 h, 4 h, 6 h) are: <0.0001, <0.0001, 0.0001, 0.0002 (*ΔdotA* vs WT); 0.0005, <0.0001, <0.0001, 0.0005 (*Δsde* vs WT); <0.0001, <0.0001, <0.0001, 0.0002 (*Δsdc* vs WT); <0.0001, <0.0001, 0.0002,

0.0035 (*Δsde/sdc* vs WT). ***p* < 0.01; ****p* < 0.001. **c** Western-blot analysis of Rab1 ubiquitination. HEK293T cells were transfected with plasmids expressing FcγRII and 3xFlag-Rab1 and then infected with the indicated *Legionella* strains for 1 h. Cell lysates were prepared and 3xFlag-Rab1 was immunoprecipitated using anti-Flag resins. Precipitated materials were analyzed by Western blot using anti-Flag or **(d)** anti-Ub antibodies. **e** Western-blot analysis 3xFlag-Rab1 after immunoprecipitation from cells challenged with indicated *Legionella* strains followed by DUB and/or DupB treatment. Source data for **b** is shown in Source Data. Data shown in **(c)**, **(d)**, and **(e)** are one representative experiment of three independent experiments. Uncropped blots are shown in Source Data.

substantially reduced after the treatment of either DUB or DupB (Fig. 1e, lanes 3 and 4). Strikingly, ubiquitinated Rab1 was completely abolished after the treatment with both enzymes (Fig. 1e, lane 5). Along this line, ubiquitinated Rab1 prepared from cells infected with *Δsde* or *Δsdc* strain was markedly reduced after DUB or DupB treatment (Fig. 1e, lane 6–11). Similarly, the reduction of ubiquitinated forms of other host substrates, such as Rab33B and LULL1 was evident after DUB or DupB treatment (Supplementary Fig. 2a, b). Together, these data demonstrated that multiple host substrates can be simultaneously ubiquitinated (via Sdc) and PR-ubiquitinated (via Sde) during *Legionella* infection. It is also worth noting that in samples from cells infected with the *Δsdc* strain, ubiquitinated Rab1 was still detected even after the DupB treatment (Fig. 1e, lane 8–11), indicating Rab1 may also be ubiquitinated by other canonical E3 ligases (see discussion below).

Ubiquitination by Sdc and Sde promotes the recruitment of host substrates and ER membranes to the LCV

Previous works indicated that Sdc and Sde were involved in recruiting ER membranes to the LCV^{24,28,44}. We hypothesized that Ub-modifications of host targets by Sdc and Sde synergistically recruit their host targets and ER membranes to the LCV. To test this hypothesis, we investigated the localization of host substrates and ER

membrane markers in infected cells. HEK293T cells expressing FcγRII and EGFP-Rab1 were challenged with WT and mutant *Legionella* strains and the localization of Rab1 was analyzed by confocal microscopy at 1 hpi (Fig. 2a, b). In cells infected with the WT strain, ~61% of the LCVs were detected positive for Rab1, while Rab1-positive LCVs were largely reduced in cells infected with the *Δsde* (-13%) or *Δsdc* (-29%) strain. More strikingly, as low as 8% of LCVs were positive for Rab1 in cells infected with the *Δsde/sdc* strain. Similar patterns were also observed for another confirmed Sdc and Sde target, LULL1 (Supplementary Fig. 3a, b). These results suggest that the LCV-recruitment of host substrates depends on the activity of both Sdc and Sde families of effectors. We next analyzed the role of Sdc and Sde in the recruitment of ER membranes to the LCV using the ER membrane marker Sec61β (Fig. 2c, d)^{28,43}. HEK293T cells expressing FcγRII and Sec61β were infected with *Legionella* strains and the recruitment of Sec61β to the LCV was examined by confocal microscopy at 2 hpi. In cells infected with WT *Legionella*, ~58% LCVs were positive for Sec61β, while in cells infected with the *Δsde*, *Δsdc*, or *Δsde/sdc* strains, the percentage of Sec61β-positive LCVs dropped to 6%, 24%, and 3%, respectively. To further validate this, we used differentiated U937 cells to quantify the LCV localization of the endogenous ER-marker Calnexin in *L. pneumophila* infection. The LCV-localization of Calnexin showed a

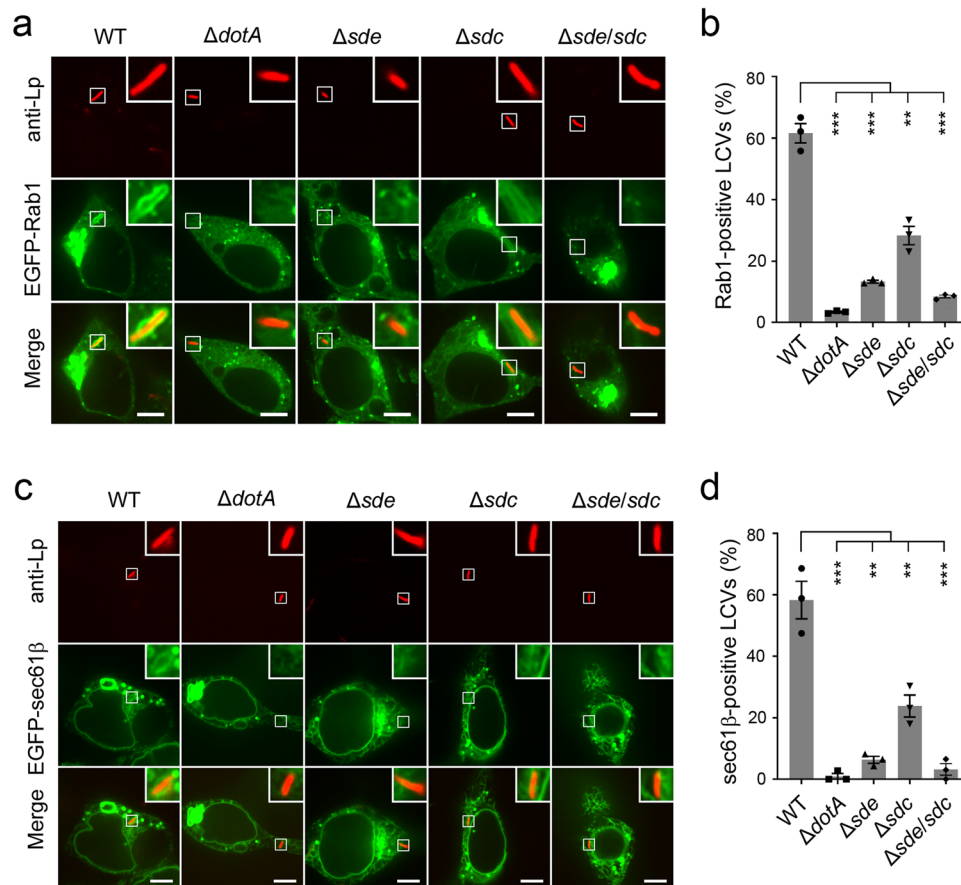


Fig. 2 | Sde and Sdc facilitate the recruitment of their host targets to the LCV.

a Representative confocal images show the localization of EGFP-Rab1 (green) in HEK293T cells challenged with specified *Legionella* strains (red) for 1 h. Scale Bar: 5 μ m. **b** Quantitative analysis of Rab1-positive LCVs in cells infected with the indicated *Legionella* strains. Data were shown as means \pm SEM of three independent experiments. At least 60 randomly selected LCVs were counted for each condition. Statistical comparisons between two groups were conducted using unpaired two-tailed Student's t-tests. The *P* values are: <0.0001 ($\Delta dotA$ vs WT); <0.0001 (Δsde vs WT); 0.0015 (Δsdc vs WT); <0.0001 ($\Delta sde/sdc$ vs WT). ***p* < 0.01; ****p* < 0.001.

c Representative confocal images show the recruitment of an ER-marker protein Sec61 β (green) at the LCV (red). Scale Bar: 5 μ m. **d** Quantitative analysis of Sec61 β -positive LCVs. Data were shown as means \pm SEM of three independent experiments. At least 60 randomly selected LCVs were counted for each condition. Statistical comparisons between two groups were conducted using unpaired two-tailed Student's t-tests. The *P* values are: 0.0007 ($\Delta dotA$ vs WT); 0.0011 (Δsde vs WT); 0.0082 (Δsdc vs WT); 0.001 ($\Delta sde/sdc$ vs WT). ***p* < 0.01; ****p* < 0.001. Source data for (b) and (d) is shown in Source Data.

similar dependency on both Sde and Sdc as observed in HEK293T cells (Supplementary Fig. 3c, d). These observations collectively indicate that Sdc and Sde family proteins are both essential for the efficient recruitment of host target proteins and ER membranes to the LCV.

Sdc and Sde build mixed Ub chains on host targets

The finding that Sdc and Sde work together to modify the same host substrate triggered us to wonder about the nature of the poly-Ub chains conjugated to host targets by Sdc and Sde. Since the Sde effectors attach mono-PR-Ub to serine residues located at flexible loops of substrate proteins^{29–32}, and the Sdc effectors catalyze canonical ubiquitination on lysine residues of substrates or a pre-conjugated Ub molecule²⁴, we hypothesized that Sdc and Sde work together to synthesize mixed Ub chains on host proteins (Fig. 3a). In this model, the Sde effectors attach a PR-Ub moiety to serine residues of the substrate while the Sdc effectors conjugate poly-Ub chains either directly to substrate lysine residues or lysine residues of the pre-conjugated PR-Ub moiety. Based on this model, we predicted that complete cleavage of the ubiquitinated substrate by a canonical DUB will yield free mono-Ub molecules in the solution while PR-Ub will remain attached to the substrate. On the other hand, treatment with DupB will specifically detach PR-Ub from the substrate and thus will

release poly-Ub chains with a variable length while canonical poly-Ub chains will remain conjugated to the substrate (Fig. 3a).

To test this hypothesis, we performed the DUB/DupB treatment experiments on ubiquitinated samples prepared both in vitro and in vivo. For the in vitro experiment, recombinant 4xFlag-Rab33B was ubiquitinated and PR-ubiquitinated by both the catalytic domain of SidC and SdeA. Rab33B was immobilized on anti-Flag resins and then treated with DUB and/or DupB. After the treatment, the supernatants were separated from the beads and both the supernatant and the bead fractions were analyzed by Western blot (Fig. 3b). As predicted, DUB treatment yielded predominantly mono-Ub in the supernatant while PR-Ub remained attached to the substrate (Fig. 3b, lanes 2 and 3). On the other hand, after DupB treatment, Ub chains with various lengths were released in the supernatant while the substrate remained partially poly-ubiquitinated (Fig. 3b, lanes 4 and 5). However, nearly all Ub moieties were released as mono-Ub from the substrate after the treatment with both the DUB and DupB (Fig. 3b, lanes 6 and 7). Similar results were obtained by the analysis of ubiquitinated Rab33B (Fig. 3c) and Rab1 (Supplementary Fig. 4) samples prepared from cells challenged with WT *L. pneumophila*. To further validate whether Sdc ubiquitinates pre-conjugated PR-Ub moieties, we first PR-ubiquitinated 4xFlag-Rab33B with V5-tagged Ub Δ GG by Sde. PR-ubiquitinated Rab33B was then ubiquitinated by SidC using WT-Ub. The final products were

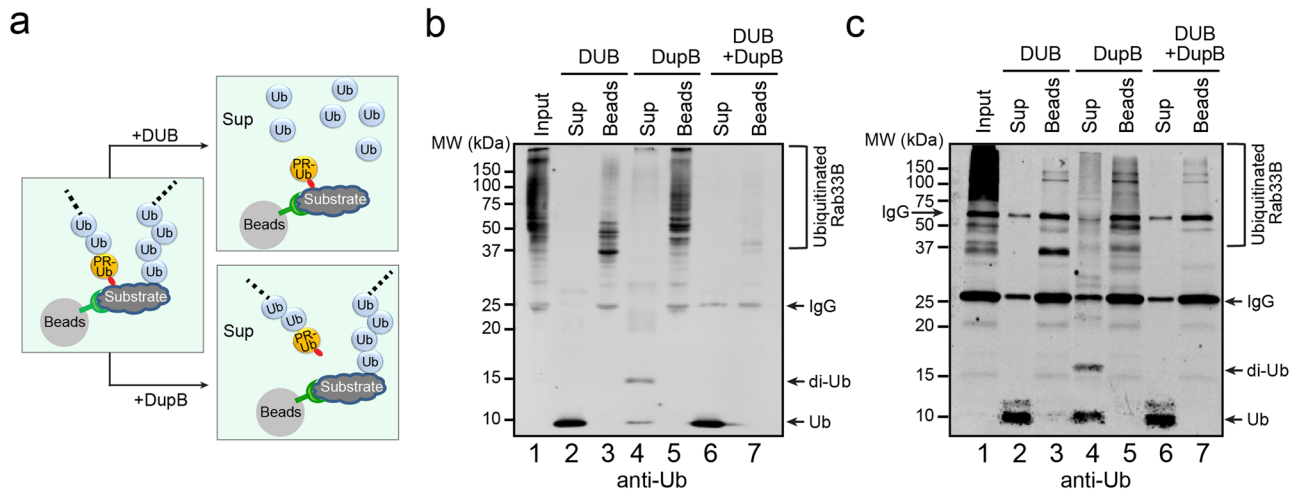


Fig. 3 | Sde and Sdc synthesize mixed ubiquitin chains on their host targets. **a** A schematic presentation of the mixed Ub chains on a substrate and the predicted outcomes after DUB or DupB cleavage. **b** Immunoblot image of in vitro ubiquitinated Rab33B after the cleavage by DUB and/or DupB. Purified recombinant 4xFlag-Rab33B was first ubiquitinated by SidC and SdeA enzymes in vitro and then immobilized on anti-Flag resins followed by the cleavage with DUB and/or DupB. The cleaved products released in the supernatant (Sup) and remained on the beads (Beads) were analyzed by SDS-PAGE followed by anti-Ub Western blot.

c Immunoblot analysis of Rab33B prepared from infected cells after the cleavage by DUB and/or DupB. HEK293T cells expressing FCγRII and 4xFlag-Rab33B were infected with wild-type *Legionella* strain for 2 h. 4xFlag-Rab33B was enriched by anti-Flag resins, followed by the treatment with DUB and/or DupB. The cleaved products that were released in the supernatant (Sup) and that remained on the beads (Beads) were analyzed by SDS-PAGE followed by anti-Ub Western blot. Data shown in (b) and (c) are one representative experiment of three independent experiments. Uncropped blots are shown in Source Data.

purified with anti-Flag resin, treated with DUB or DupB, and analyzed by anti-V5 Western blot. Following DupB treatment, di-Ub (and possibly poly-Ub) chains positive for V5 were released from Rab33B (Supplementary Fig. 5, lane 4), indicating that the pre-conjugated PR-Ub moieties can indeed be ubiquitinated by Sdc. Taken together, these results demonstrated that Sdc and Sde work together to build mixed Ub chains on host substrates.

The poly-Ub chains synthesized by Sdc and Sde prevent the recognition by autophagy adaptor p62

The LCV was enriched with ubiquitinated species at both early and late time points of the infection cycle, however, previous studies showed that Ub-binding autophagy adaptors were excluded from the LCV, and the exclusion depended on the Sde family members³⁶. To investigate the mechanism of the avoidance of autophagy adaptor recognition by the Ub-positive LCV, we examined p62 recruitment at the LCV in *Legionella*-challenged cells and the interaction between p62 and host proteins ubiquitinated by Sdc and Sde. HEK293T cells expressing FCγRII and mCherry-p62 were infected with *L. pneumophila* strains. Although most LCVs were positive for Ub signals at 1 hpi (Fig. 1a, b), a very low percentage (~4%) of LCVs were detected positive for p62 (Fig. 4a, b). Almost no LCVs were positive for p62 in cells infected with the $\Delta dotA$ or Δsdc strain. However, in cells challenged with the Δsde strain, up to 40% of the LCVs were positive for p62 at 1 hpi (Fig. 4a, b), although the percentage of LCVs positive for Ub was reduced by more than 2-fold compared to the infection with the WT strain (Fig. 1a, b). The p62-positive vacuoles decreased at later infection times (Fig. 4b), correlating with decreased Ub signals at the LCV (Fig. 1b and Supplementary Fig. 6a, b). The ability to suppress p62 recruitment to the LCV was fully restored when the Δsde strain was supplemented with a plasmid expressing WT SdeA (Fig. 4a, b) regardless of the high percentage (>80%) of Ub-positive LCVs (Supplementary Fig. 6a, b). Surprisingly, the ability to suppress p62 recruitment to the LCV was also fully restored when the Δsde strain was introduced to express the SdeA_{H277A} mutant, which is able to ADP-ribosylate Ub but is defective in PR-Ub ligation, but not the SdeA_{EE/AA} mutant, which is defective in its mART activity (Fig. 4a, b). It is worth noting that cells infected with the Δsde +pSdeA_{H277A} strain exhibited a higher percentage of Ub-positive

LCVs (48%) than with the Δsde +pSdeA_{EE/AA} strain (33%) after 1 h of infection (Supplementary Fig. 6a, b) indicating that p62 recruitment does not correlate with the amount of Ub species at the LCV. Together, these results let us hypothesize that the observed suppression of p62 recruitment to the LCV is likely attributed to the failure of the direct binding of p62 with the ubiquitinated species generated by Sdc and Sde.

To test this hypothesis, we examined the interaction between p62 and ubiquitinated substrates enriched from cells infected with *L. pneumophila*. HEK293T cells expressing FCγRII, 3xFlag-Rab1, and HA-p62 were challenged with *Legionella* strains for 1 h. 3xFlag-Rab1 was immunoprecipitated with anti-Flag resins and the immunoprecipitated materials were analyzed by Western blot. In agreement with the p62 recruitment assay (Fig. 4a), HA-p62 was co-immunoprecipitated with the Rab1 proteins from cells infected with the Δsde strain or the Δsde strain supplemented with a plasmid expressing the SdeA_{EE/AA} mutant, but not the WT, $\Delta dotA$, or the Δsdc strain introduced to express either WT SdeA or the SdeA_{H277A} mutant (Fig. 4c, d). Similar results were obtained by an in vitro pull-down assay (Supplementary Fig. 7). GFP-fused recombinant proteins of the Ub-associated (UBA) domain of p62 were purified and immobilized to GFP-nanobody resins to pull down ubiquitinated Rab33B. Rab33B proteins ubiquitinated by SidC alone were effectively pulled down by GFP-UBA_{p62}, however, the interaction between GFP-UBA_{p62} and Rab33B ubiquitinated by both SidC and SdeA was markedly reduced. More strikingly, the interaction was nearly completely abolished when the Rab33B proteins were ubiquitinated by both SidC and the SdeA_{H277A} mutant (Supplementary Fig. 7). These data confirmed that the poly-Ub chains synthesized by Sdc and Sde are unsusceptible to the recognition by autophagy receptor p62. This observation allowed us to postulate that the disruption of the interaction between the UBA_{p62} domain with poly-Ub chains may be caused by the modification at Ub R42 with a phosphoribose (PR) (by WT SdeA) or an ADP-ribose (ADPR) group (by SdeA_{H277A} mutant). In fact, it has been shown that the UBA domain binds Ub at the I44 hydrophobic patch, with R42 in its proximity⁴⁵. The presence of PR or ADPR modification on R42 will likely cause steric collision against the binding with the UBA_{p62} domain (Fig. 4e).

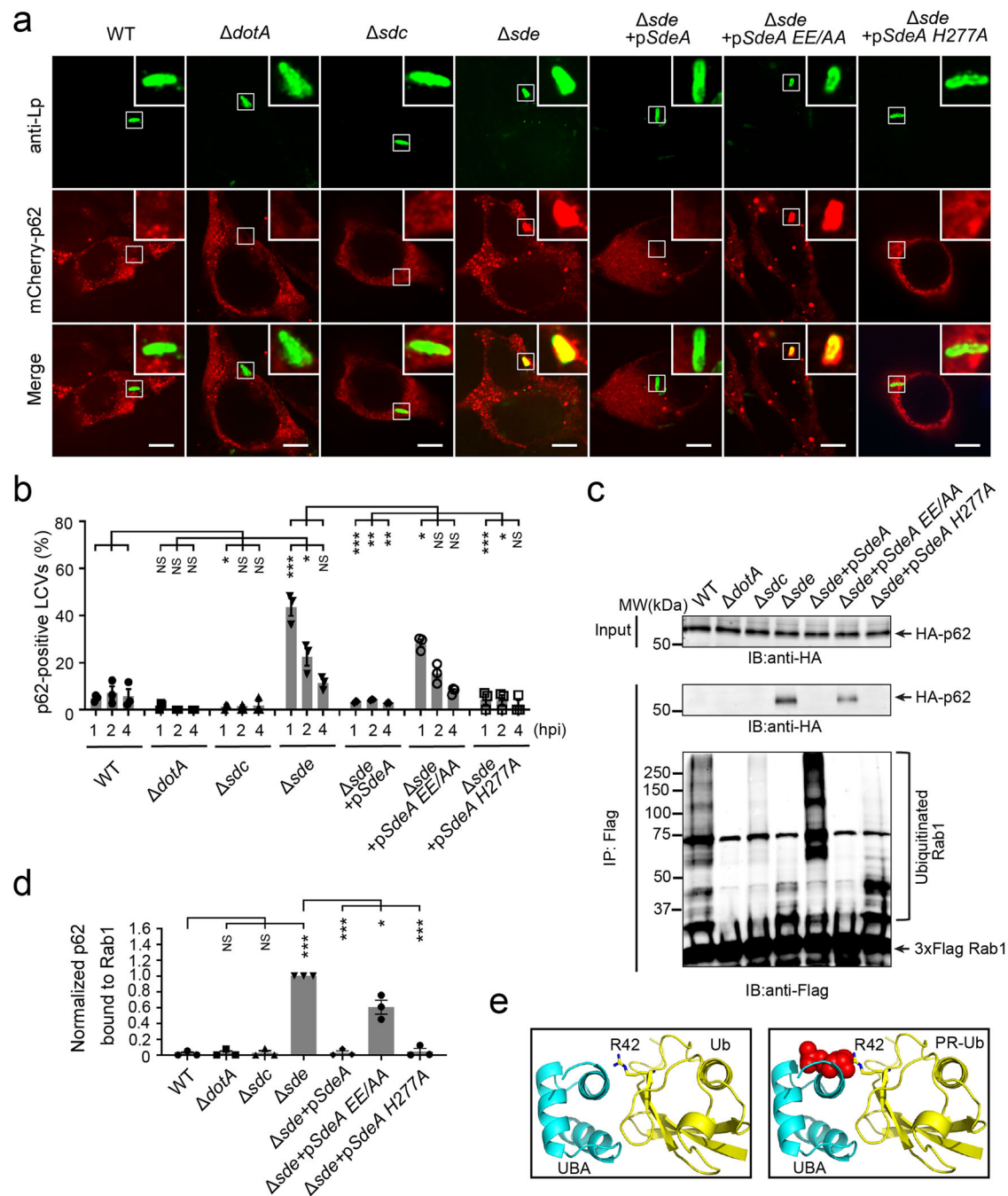
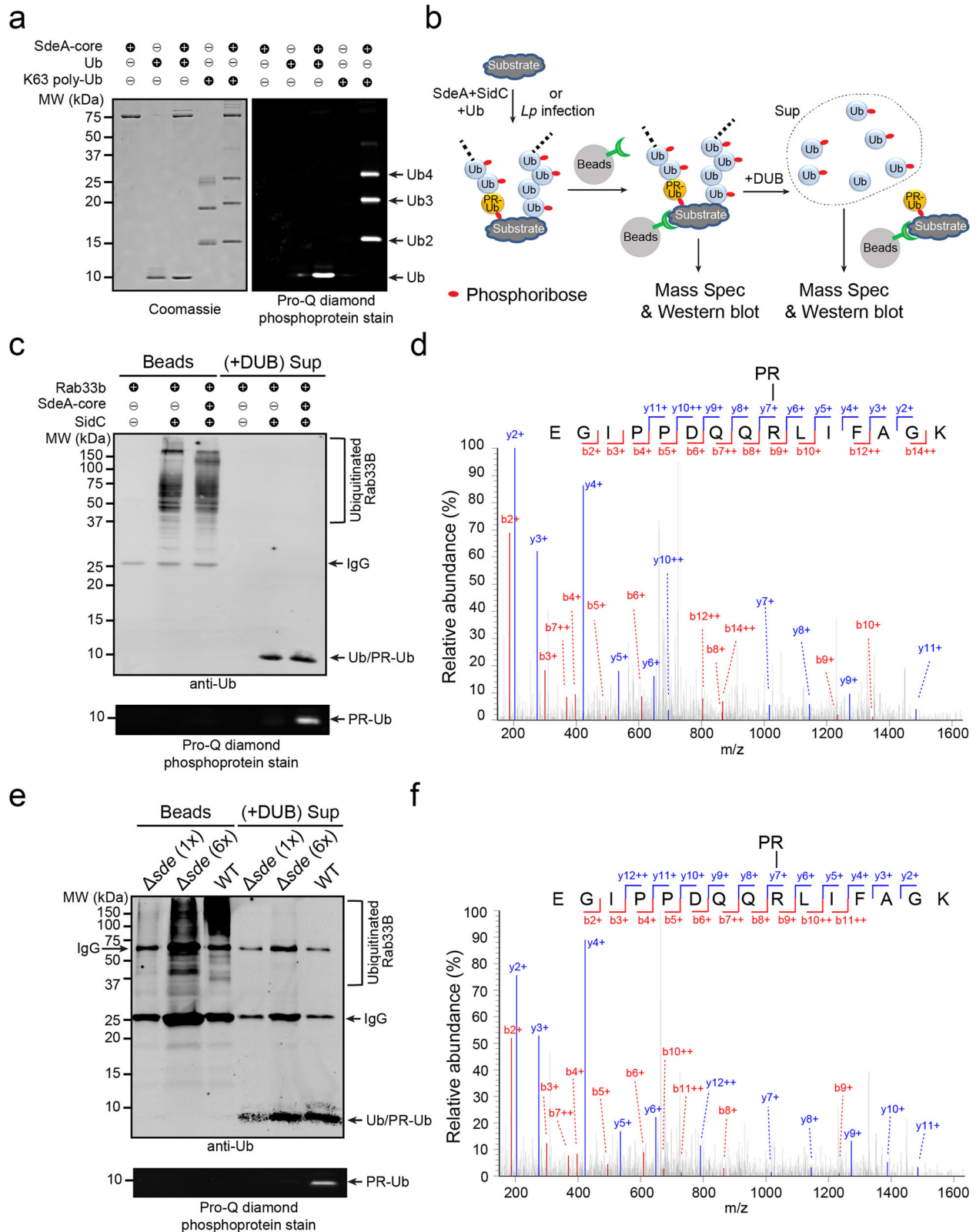


Fig. 4 | Sde suppresses the recruitment of p62 to the LCV by disrupting the physical interaction between p62 and Ub.

a Representative confocal images show the localization of mCherry-p62 (red) in HEK293T cells challenged with specified *Legionella* strains (green) for 1 h. Scale Bar: 5 μ m. **b** Quantitative analysis of p62-positive LCVs in cells infected with the indicated *Legionella* strains. Data were shown as means \pm SEM of three independent experiments. At least 33 randomly selected LCVs were counted for each condition. Statistical comparisons between two groups were conducted using unpaired two-tailed Student's *t*-tests. The *P* values (1 h, 2 h, 4 h) are: 0.0547, 0.0651, 0.1212 ($\Delta dotA$ vs WT); 0.0473, 0.0937, 0.318 (Δsdc vs WT); 0.0005, 0.0304, 0.1779 (Δsde vs WT); 0.0004, 0.008, 0.0065, (Δsde +pSdeA vs Δsde); 0.0204, 0.1862, 0.1343 (Δsde +pSdeA_{EE/AA}); 0.0008, 0.0126, 0.0243 (Δsde +pSdeA_{H277A}). NS = nonsignificance; **p* < 0.05; ***p* < 0.01; ****p* < 0.001. **c** Co-immunoprecipitation assay of the interaction between p62 and ubiquitinated Rab1. HEK293T cells expressing FcγRII, 3xFlag-Rab1, and HA-p62 were infected with the indicated *Legionella* strains for 1 h. 3xFlag-Rab1 was enriched by anti-Flag

immunoprecipitation. Immunoprecipitated materials were analyzed by anti-Flag (Rab1) and anti-HA (p62) Western blot. **d** The amount of HA-p62 bound to Rab1 was normalized to the value of Δsde group. Data were shown as means \pm SEM of three independent experiments. Statistical comparisons between two groups was conducted using unpaired two-tailed Student's *t*-tests. The *P* values are: 0.8082 ($\Delta dotA$ vs WT); 0.7847 (Δsdc vs WT); <0.0001 (Δsde vs WT); <0.0001 (Δsde +pSdeA vs Δsde); 0.0108 (Δsde + pSdeA_{EE/AA}); <0.0001 (Δsde + pSdeA_{H277A}). NS nonsignificance; **p* < 0.05; ****p* < 0.001. **e** Ribbon diagrams of the UBA-Ub complex (PDB ID: 2g3q) and the modeled UBA-PR-Ub complex. The UBA domain is colored in blue and the Ub is in yellow. The PR group attached to Ub R42 is shown in red spheres. Note the steric collision between the UBA domain and the PR group. This figure was generated using PyMol. Source data for (**b**) and (**d**) is shown in Source Data. Data shown in (**c**) is one representative experiment of three independent experiments. Uncropped blots are shown in Source Data.



The poly-Ub chains synthesized by Sdc and Sde are phosphoribosylated by Sde

To examine whether poly-Ub chains can be modified by Sde, we analyzed the modification on Ub using both biochemical and mass spectrometry approaches. First, K63-linked poly-Ub chains were treated with SdeA Core-WT, which contains functional mART and PDE domains. The phosphoribosyl modification on Ub moieties can be

detected by SDS-PAGE followed by Pro-Q diamond phosphoprotein stain (Fig. 5a), which specifically stains exposed phosphoryl groups⁴⁶. This result demonstrated that free poly-Ub chains can be phosphoribosylated by Sde. To address whether internal Ub moieties can be modified by Sde, we synthesized tri-Ub chains, each of which contains two Ub-R42K mutants and one WT-Ub at either the distal, internal, or proximal position. These tri-Ub chains were modified by SdeA, and

Fig. 5 | Sde modifies poly-Ub chains by phosphoribosylation. **a** In vitro modification of K63-linked poly-Ub chains by SdeA. Mono-Ub or K63-linked poly-Ub chains were incubated with the catalytic core of SdeA and NAD⁺. The products were analyzed by SDS-PAGE followed by staining with Coomassie blue (left panel) or Pro-Q diamond (right panel). **b** Schematic diagram of the poly-Ub chains attached to the substrate and experimental flow of biochemical and Mass spectrometry analysis of the poly-Ub chains. **c** Biochemical analysis of Ub modification by Sde in vitro. Recombinant 4x-Flag-Rab33B was ubiquitinated in vitro by the catalytic domain of SidC or by both SidC and SdeA. Ubiquitinated Rab33B was immobilized on anti-Flag beads and treated with a canonical DUB. The samples before and after the DUB treatment were analyzed by SDS-PAGE followed by anti-Ub Western blot (top panel) or by Pro-Q diamond stain (bottom panel). **d** LC-MS/MS spectrum of a Ub peptide from an in vitro ubiquitinated sample showing the phosphoribosyl modification at Ub R42. Recombinant 4x-Flag Rab33B was ubiquitinated in vitro by

SidC and SdeA and then enriched by anti-Flag beads. The resulting bound proteins were treated with a purified DUB, and the Ub molecules released from the cleavage were analyzed by LC-MS/MS. **e** Biochemical analysis of Ub modification by Sde in vivo. HEK293T cells expressing FCyRII and 4xFlag-Rab33B were infected with WT or Δ sde strain for 2 h. 4xFlag-Rab33B was immunoprecipitated by anti-Flag resins and then treated with a canonical DUB. The samples before and after the DUB treatment were analyzed by SDS-PAGE followed by anti-Ub Western blot (top panel) or by Pro-Q diamond stain (bottom panel). Samples prepared from cells infected with the Δ sde strain were loaded with 1 fold (1x) or 6 folds (6x) of the amount of the sample from the WT infection. **f** LC-MS/MS spectrum of a Ub peptide from a sample prepared from *Legionella* infected cells showing the phosphoribosyl modification at Ub R42. Samples were prepared similarly as in (e). Data shown in (a), (c), and (e) are one representative experiment of three independent experiments. Uncropped gels and blots are shown in Source Data.

signals for the phosphoribosyl group were detected for all three tri-Ub chains by Pro-Q diamond phosphoprotein stain (Supplementary Fig. 8). These results confirm that internal Ub moieties within a poly-Ub chain can be phosphoribosylated by Sde.

Next, we asked whether poly-Ub chains attached to a substrate by Sdc and Sde are also modified with phosphoribose. To answer this question, we prepared ubiquitinated substrates both in vitro using recombinant SidC and SdeA enzymes and in vivo from *Legionella*-infected cells. The ubiquitinated substrates were either directly analyzed by MS/MS or digested with a canonical DUB (the N-terminal domain of SdeA) followed by MS/MS analysis of the released free Ub (Fig. 5b). For the in vitro experiment, recombinant 4xFlag-Rab33B was ubiquitinated by SidC or by both SidC and SdeA. Ubiquitinated Rab33B was then treated with DUB and the supernatant samples were separated by SDS page and analyzed by anti-Ub Western blot and Pro-Q diamond phosphoprotein stain. PR-Ub was only detected in the supernatant from the sample ubiquitinated by both SidC and SdeA but not by SidC alone (Fig. 5c). Phosphoribosyl modification on Ub moieties within the Ub chains synthesized by SidC and SdeA in vitro was further verified by MS/MS analysis. An additional mass of 201.009 Da, corresponding to a phosphoribosyl group was detected at Ub R42 (Fig. 5d). We next examined the modification on Ub moieties from poly-ubiquitinated substrates under infection conditions (Fig. 5e). FcyRII and 4xFlag-Rab33B-expressing HEK293T cells were infected with WT or Δ sde *Legionella* strains for 2 h. Ubiquitinated Rab33B was immunoprecipitated with anti-Flag resins. Following a similar procedure described above, PR-Ub molecules were only detected from samples originating from cells infected with the WT but not the Δ sde strain (Fig. 5e, f). Phosphoribosyl modification can also be detected in both in vitro and in vivo ubiquitinated samples by MS/MS without the DUB treatment (Supplementary Fig. 9a, c). Interestingly, we also detected Ub chain linkages in these samples. In agreement with the previously reported results²⁴, we found that SidC prefers to catalyze K63, K48, and K33 Ub chains (Supplementary Fig. 9b, d). Taken together, our results demonstrated that the Ub moieties within the poly-Ub chains synthesized by Sdc and Sde are phosphoribosylated by Sde.

The PR-Ub-specific deubiquitinases, DupA and DupB can process ADPR-Ub to PR-Ub on internal Ub moieties of poly-Ub chains

The phosphoribosyl modification of Ub is a two-step reaction, of which the first step involves ADP-ribosylation on Ub by the Sde mART activity, and the second step involves the hydrolysis of ADPR to PR with the releasing of an AMP molecule. Our previous results showed that several PDE domain-containing effectors, including the PR-Ub specific deubiquitinases, DupA and DupB, were able to process mono-ADPR-Ub to PR-Ub⁴⁴. We thus asked whether DupA and DupB contribute to the cleavage of ADPR to PR on poly-Ub chains. To answer this question, free poly-Ub chains were first ADP-ribosylated by SdeA-Core H227A mutant and then treated with either DupA or DupB (Fig. 6a). In

contrast to the untreated, samples treated with either DupA or DupB exhibited positive signals upon Pro-Q Diamond stain, indicating that both DupA and DupB can cleave ADPR to PR that is attached to Ub moieties within the poly-Ub chain (Fig. 6b).

Beyond free poly-Ub chains, DupA and DupB were also capable of processing ADPR-Ub to PR-Ub on poly-ubiquitinated substrates. Ubiquitinated Rab33B was generated in the presence of SidC and SdeA-Core H227A and the product was then treated with either DupA or DupB. The Ub moieties were then released from the substrate by treatment with DUB and analyzed SDS-PAGE followed by Pro-Q Diamond stain (Fig. 6c). PR-Ub was detected from DupA or DupB-treated samples but not from untreated ones (Fig. 6d). Collectively, these results indicate that the previously identified PR-Ub specific deubiquitinases, DupA and DupB, may also be involved in the phosphoribosyl modification of poly-Ub chains by processing ADPR to PR.

Cross-linking of multiple Sdc and Sde targets by canonical and PR-ubiquitination

The Sde family effectors conjugate mono-Ub to a substrate through a two-step reaction, namely PR-ubiquitination. We showed that Sde effectors also ADP-ribosylate internal Ubs within the poly-Ub chains. Although some of the ADPR groups can be further processed into PR by Sde or DupA/DupB, it is legitimate that some of the internal Ubs within the poly-Ub chain attached to one substrate can also be conjugated to a second substrate through PR-ubiquitination by Sde. In this way, multiple host targets can be covalently cross-linked to one poly-Ub chain created by Sdc and Sde (Fig. 7a). To test this hypothesis, we infected cells expressing two known Sdc and Sde substrates, 3xFlag-Rab1 and HA-Rab33B, with WT or mutant *Legionella* strains. Cell lysates were prepared after 2 hpi followed by immunoprecipitation with anti-Flag resins and analyzed by both anti-Flag (Fig. 7b) and anti-HA (Fig. 7c) Western blot. High molecular weight bands positive for both Rab1 (Fig. 7b, lane 4) and Rab33B (Fig. 7c, lane 4) were detected in samples from cells infected with the WT strain but not from uninfected cells or cells infected with Δ sde (Fig. 7b, c, lanes 1 and 2). These high molecular weight bands were markedly reduced in samples from cells infected with the Δ sdc strain (Fig. 7b, c, lane 3). These observations suggest that Rab33B and Rab1 were cross-linked to form the high molecular weight species allowing the co-immunoprecipitation of Rab33B with Rab1. To elucidate the nature of the cross-linking, the immunoprecipitated samples from cells infected with the WT strain were treated with DUB or DupB and analyzed by Western blot. As expected (Fig. 7a), after DUB treatment, the high molecular weight bands corresponding to cross-linked species were eliminated and resulted in unmodified and PR-ubiquitinated (mono- or multiple mono-) Rab1 (Fig. 7b, lane 5) and Rab33B (Fig. 7c, lane 5). Accordingly, DupB treatment resulted in unmodified and poly-ubiquitinated (with variable lengths) Rab1 (Fig. 7b, lane 6) and Rab33B (Fig. 7c, lane 6). Cross-linking between Rab1 and Rab33B was further verified using samples prepared by reversed immunoprecipitation with anti-HA resins (Supplementary

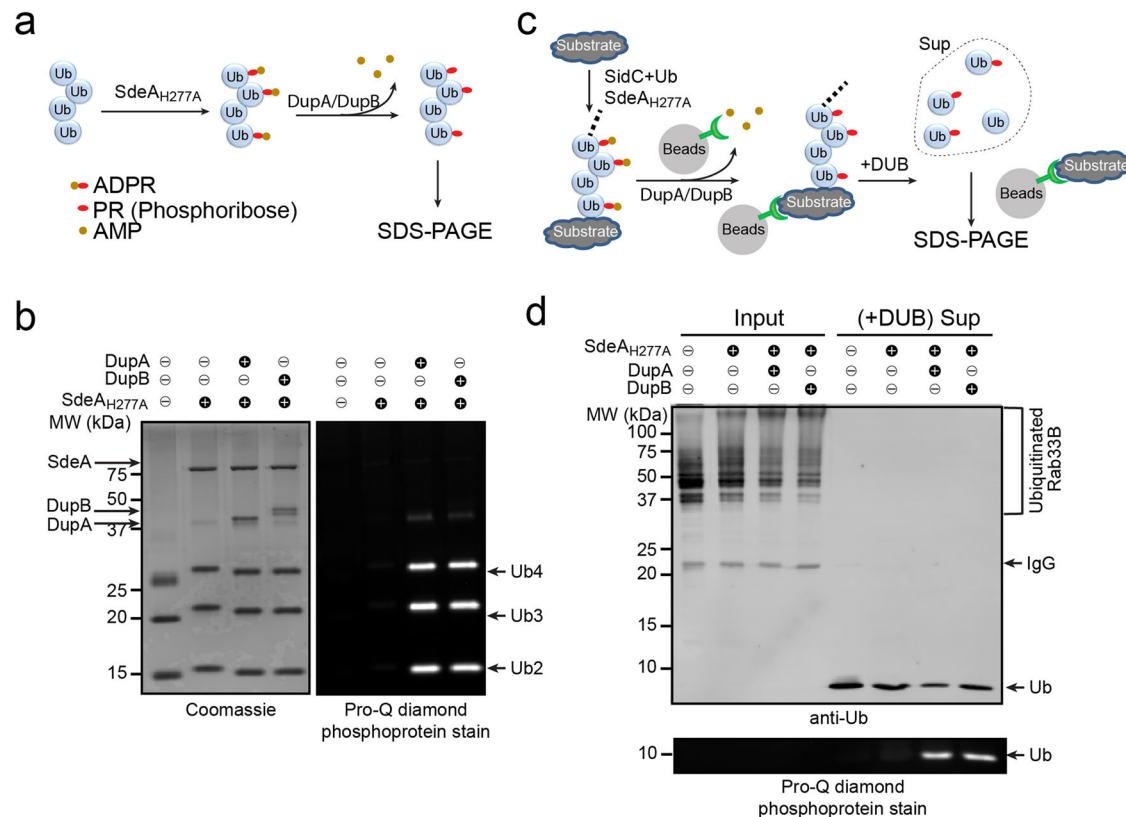


Fig. 6 | Both DupA and DupB play a role in the processing of ADPR-Ub to PR-Ub.

a Schematic representation of DupA and DupB modification on free poly-Ub chains. **b** K63-linked poly-Ub chains were first modified by purified SdeA_{H277A} and subsequently treated with DupA or DupB. Conversion of ADPR-Ub to PR-Ub following DupA or DupB treatment was analyzed by SDS-PAGE followed by Coomassie blue (left panel) or Pro-Q diamond stain (right panel). **c** Schematic representation of DupA and DupB modification on a poly-ubiquitinated substrate. **d** 4x-Flag Rab33B

was poly-ubiquitinated by recombinant SidC and modified by SdeA_{H277A}. Ubiquitinated Rab33B was immobilized on anti-Flag beads and then treated with DupA or DupB. The samples were then treated with a canonical DUB to release mono-Ub. Samples before and after DUB cleavage were analyzed by SDS-PAGE followed by anti-Ub Western blot (top panel) or by Pro-Q diamond stain (bottom panel). Data shown in **(b)** and **(d)** are one representative experiment of three independent experiments. Uncropped gels and blots are shown in Source Data.

Fig. 10a). Furthermore, cross-linking of Sdc and Sde substrates in *Legionella* infection was also observed between other host targets (for example, between Rab1 and LULL1, Supplementary Fig. 10b, c). Together, these results demonstrated that multiple host targets were cross-linked through unconventional Ub chains generated by Sde and Sdc at the LCV.

Discussion

In this study, we reported a coordinated interplay between two families of Ub-hijacking effectors, the Sdc family effectors, which mimic host E3 ligases and catalyze canonical poly-ubiquitination, and the Sde effectors, which catalyze unconventional phosphoribosyl-linked serine ubiquitination (PR-ubiquitination) on host targets. Our data support a model of poly-Ub chains built by these two families of effectors around the LCV (Fig. 7d). In this model, the translocated Sdc ligases catalyze canonical poly-ubiquitination either directly to host proteins or to a PR-Ub molecule that is attached to the same host protein by Sde. Furthermore, the Sde effectors modify Ub moieties within the poly-Ub chain via ADP-ribosylation and the attached ADP-ribose group can be further processed into phosphoribose (PR) by the PDE domain of Sde or DupA/DupB, two previously identified PR-Ub specific deubiquitinases. Interestingly, the internal ADP-ribosylated Ub moieties can also be conjugated to other host substrates through PR-ubiquitination by the PDE domain of Sde. In this way, two or more Sdc and Sde substrates can be conjugated to the same poly-Ub chain (Fig. 7d). Thus a Ub-coat containing unconventionally modified Ub chains was built around the LCV by the *Legionella* bacterium.

An apparent paradox associated with the Ub-coat at the LCV is that the Ub signals do not trigger autophagy clearance of the bacterium. It has been postulated that potential *cis*-acting effectors may modify the Ub-coat and hence disrupt the recruitment of autophagy adaptors to the LCV³⁶. Surprisingly, a recent publication reported that the exclusion of p62 from the LCV was due to Sde-mediated PR-ubiquitination of host Ubiquitin-Specific Protease 14 (USP14), which disrupted the direct interaction between USP14 and p62⁴⁷. However, this report ignored the fact that the LCV surface is enriched with Ub species nearly throughout the *L. pneumophila* infection cycle^{21,22} and the fact that Ub chains are the major driving force for the recruitment of autophagy adaptors, such as p62^{8,48}. USP14 knockdown could not explain the exclusion of p62 from the Ub-enriched LCV. More importantly, our data showed that p62 was excluded from the LCV when host cells were infected with the $\Delta sde+pSdeA_{H277A}$ strain, which is unable to PR-ubiquitinate any host targets but only modifies Ub by ADP-ribosylation (Fig. 4a–c). Thus, PR-ubiquitination of host substrates per se does not account for the exclusion of p62. Here we provided direct evidence to support the Ub-coat modification model. We showed that the Sde family effectors are the *cis* factors that modify the Ub moieties within the Ub chains, and Sde modification results in the disruption of the Ub adaptor-interacting surface on Ub molecules and hence prevents the recruitment of host autophagy adaptors to the LCV. This model is further supported by the results reported in the concomitantly submitted manuscript by Kotewicz et al.⁴⁹

Our studies revealed the structural nature of the unconventional poly-Ub chains created at the LCV. However, it is intriguing to

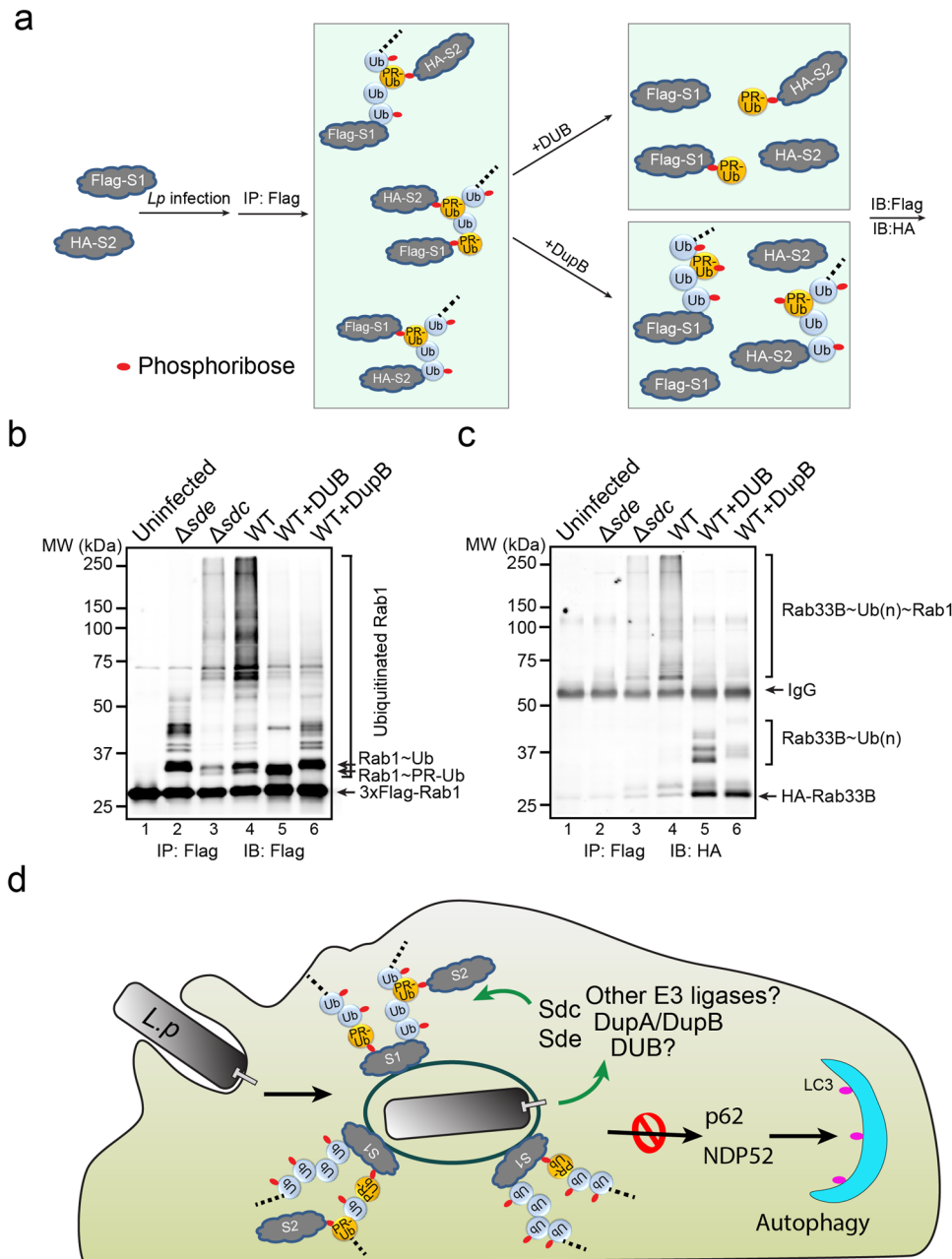


Fig. 7 | Cross-linking of multiple Sdc and Sde targets by canonical and PR-ubiquitination. **a** Schematic model of two host substrates that are cross-linked by canonical and PR-ubiquitination and the experimental flow of verification. In this model, a poly-Ub chain attached to one substrate (either through canonical or PR-ubiquitination), and the Ub moieties within the Ub chain can be used to modify a second substrate via PR-ubiquitination. The cleavage by a canonical DUB will result in unmodified and mono- or multi-mono PR-ubiquitinated products, while the cleavage by DupB will yield unmodified and ubiquitinated (with a variable length) products. **b, c** Biochemical analysis of substrate cross-linking in *Legionella*

infection. HEK293T cells expressing FCyRII, 3xFlag-Rab1, and HA-Rab33B were infected with indicated *Legionella* strains for 2 h. 3xFlag-Rab1 was immunoprecipitated by anti-Flag resins and then treated with a canonical DUB or DupB. The samples before and after the treatment were analyzed by SDS-PAGE followed by anti-Flag (**b**) or anti-HA Western blot (**c**). **d** A schematic model of unconventional poly-Ub chains at the LCV serving as a scaffold for cross-linking multiple host targets and preventing host autophagy detection. Data shown in (**b**) and (**c**) are one representative experiment of three independent experiments. Uncropped blots are shown in Source Data.

contemplate how the Ub-coat around the LCV benefits *Legionella* infection. It has been reported that as soon as 15 minutes after bacterial uptake, the LCV is covered by ER-derived vesicle and enriched with ER residential proteins^{50,51}. The recruitment of ER vesicles has been attributed to the manipulation of host small-GTPases, such as Rab1⁵², Rab33B, and Rab6A⁵³, by *Legionella* effectors. Here we showed that both Sdc and Sde effectors are required for the recruitment of their host targets and ER markers Sec61 β (Fig. 2) and HDEL²⁴ to the LCV, suggesting canonical ubiquitination and PR-ubiquitination are critical

in the accumulation of ER materials at the LCV. One explanation for ER vesicle recruitment to the LCV is that Sdc and Sde modify key host factors that control Golgi-to-ER trafficking, which causes altered functions of these host factors and results in the association of the LCV with the ER. Alternatively, PR-ubiquitination of ER proteins may disrupt ER integrity and cause fragmentation, facilitating the recruitment of ER-derived vesicles and associated proteins to the LCV⁴³. However, given the fact that many ER proteins were found to be PR-ubiquitinated after *Legionella* infection^{43,44} and our data showing the cross-linking of

multiple host substrates to the poly-Ub chains generated by Sdc and Sde, the association of ER-derived vesicles with the LCV can be explained by an alternative mechanism. It is possible that the poly-Ub chains synthesized by Sdc and Sde provide multiple anchoring points to covalently crosslink proteins associated with either the LCV or ER vesicles and thus to tether together these two types of membrane bound vesicles. To further unravel the physiological role of the Ub-coat at the LCV is certainly an exciting future direction.

In this study, we reported that the Sdc and Sde families of effectors contribute to the creation of poly-Ub chains at the LCV. Furthermore, we also provided evidence to support that the PR-Ub-specific deubiquitinases, DupA and DupB, may also be involved in the poly-Ub chain assembly by processing ADPR to PR. However, *Legionella pneumophila* encodes a large number of effectors that hijack the host Ub system^{54–58} and it is intriguing to ask whether other *Legionella* Ub-hijacking effectors are involved in the building of the Ub-coat. It is notable that when cells were infected with the Δ sdc strain, ubiquitinated Rab1 was detected even after the treatment with DupB (Fig. 1e), indicating Rab1 can also be ubiquitinated by other E3 ligases. However, the Ub signals at the LCV were significantly reduced in cells infected with the Δ sdc strain (Fig. 1a, b), suggesting Sdc effectors are the major E3 ligases for the building of the Ub-coat at the LCV. Besides E3 ligases, *Legionella pneumophila* also encodes several effectors that function as a canonical DUB^{25,59–64}. At least some of these DUBs have been shown to regulate overall ubiquitination at the LCV^{25,59,61,62}. Interestingly, the N-terminal DUB domain of Sde family of effectors also contribute to the Ub species at the LCV⁴⁹. In this study, although we showed that the Sdc and Sde families of Ub ligases are the major players, other E3 ligases and DUBs may also be involved in either the establishment or the dynamics of the Ub-coat at the LCV. For example, the F-box-containing E3 Ub ligase AnkB was previously shown to poly-ubiquitinate host proteins, leading to their degradation and the subsequent generation of amino acids used by the bacteria during infection^{65–67}. Like Sdc, this effector may also contribute to the accumulation of ubiquitinated species detected at the LCV. Nevertheless, elucidating the physiological roles of each player in the Ub-coat requires more delicate experiments in the future.

In summary, we presented the results to show two distinct family Ub E3 ligases, Sdc and Sde work together to assemble a Ub-coat at the LCV during *Legionella* infection. This Ub-coat contains unconventional mixed Ub chains with internal Ub moieties modified with a phosphoribosyl group. This modification is important to prevent the recognition autophagy adaptors, such as p62. Our results elucidate the nature of the Ub-coat and provide a molecular mechanism for the avoidance of autophagy adaptors and therefore the protection of the LCV from xenophagy clearance.

Methods

Cloning and mutagenesis

Plasmids used for expression in mammalian cells, EGFP-Rab1, 4xFlag-Rab33B, LULL1-HA, and HA-Ub were generated in previous studies^{24,44}. To generate 3xFlag-Rab1, Rab1 was amplified from EGFP-Rab1, digested with EcoRI and BamHI, and inserted into pCMV 3xFlag 7.1 vector digested with the same restriction enzymes. To generate EGFP-3xFlag-Rab1, 3xFlag-Rab1 fragment was amplified, digested with BamHI and XhoI, then inserted into pEGFP-C1 vector digested with BglIII and Sall. To generate EGFP-sec61 β , a fragment of EGFP was PCR amplified, digested with NheI and BspEI, and then inserted into pTagBFP-sec61 β obtained from Dr. Fenghua Hu (Cornell University) and digested with the same restriction enzymes. HA-p62 and mCherry-p62 were also obtained from Dr. Fenghua Hu (Cornell University). Flag-Syntaxin 17 was purchased from Addgene (Addgene #19506).

For plasmids used for *Legionella* expression, DNA fragments of wild-type and mutants of SidC and SdeA were amplified from plasmids for mammalian expression^{24,44}, and digested with BamHI and XhoI. The

digested DNA fragment was inserted into pZL507 plasmid obtained from Dr. Zhao-Qing Luo (Purdue University) and digested with BamHI and Sall. To delete sdcA-sidC genes in Δ sdc strain, DNA fragments of 1.2 Kb upstream and 1.2 Kb downstream of the sdc (*sdcA-sidC*) gene loci were PCR amplified and cloned into the pSR47s vector obtained from Dr. Zhao-Qing Luo (Purdue University), to generate pSR47s- Δ sdc plasmid.

Plasmids used for protein expression in *E. coli*, SidC (aa.1-542), Ubch7, Ub WT and mutants, 4xFlag-Rab33B, DupA, DupB, human E1, His-TEV-Ub K6, Ubc13, and Mms2 were generated in previous studies^{24,44,68,69}. To generate V5-tagged Ub Δ GG, DNA fragment of human Ub 1-74 carrying an N-terminal short V5 tag (GKPIPPLLGLD) was PCR amplified from pET21a-Ub WT, digested with NdeI and XhoI. The digested DNA fragment was inserted into pET21a vector digested with the same restriction enzymes. DNA fragments corresponding to the DUB domain of SdeA (aa.1-213) and SdeA-Core (aa.231-925) were PCR amplified from genomic DNA of *L. pneumophila* Philadelphia strain and digested with BamHI and XhoI. The corresponding DNA fragments were ligated into pET28a 6xHis-Sumo digested vector with the same restriction enzymes. Site-directed mutagenesis was performed with overlapping primers to generate the SdeA-Core H277A mutant. Constructs for 6xHis-Mms2, GST-Ubc13, GST-Yuh1, Ub_{K63R}, and Ub_{D77} were a gift from Dr. Scott Emr (Cornell University). To generate GFP-UBA_{p62}, the UBA domain of p62 (aa. 382-436) was PCR amplified from mCherry-p62 and digested with BamHI and XhoI. The digested DNA fragment was inserted into pET28a 6xHis-GFP vector digested with the same restriction enzymes.

Protein expression and purification

All Bacterial expression constructs were transformed into *Escherichia coli* Rosetta (DE3) cells. Cultures from single colonies were grown in Luria-Bertani (LB) medium containing 50 μ g/ml of kanamycin or 100 μ g/ml of ampicillin to a density between 0.6 and 0.8 OD₆₀₀. Protein expression was induced with 0.2 mM isopropyl-B-D-thiogalactopyranoside (IPTG) at 18 °C overnight. Harvested cells were resuspended in lysis buffer (20 mM Tris-HCl pH 7.5, and 150 mM NaCl) and lysed by sonication. The lysates were clarified by centrifugation at 31,000 \times g for 45 min at 4 °C, and the supernatant was incubated with cobalt resin (Gold-Bio; for His-tagged proteins) or glutathione Sepharose 4 Fast Flow resin (GE; for GST-tagged proteins) for 1.5 h at 4 °C. Bound proteins were washed extensively with lysis buffer. The SUMO-specific protease Ulp1 was added to the resin slurry to release the protein from the His-SUMO tag and resin. Eluted proteins were further purified by fast protein liquid chromatography (FPLC) size exclusion chromatography using either a Superdex S75 or S200 columns (GE Life Sciences). Peak fractions were then collected and concentrated. 6xHis-tagged GFP-UBA_{p62} cells were sonicated in lysis buffer (20 mM Tris-HCl pH 7.5 and 150 mM NaCl), cleared by centrifugation at 31,000 \times g for 45 min at 4 °C, and incubated with cobalt resin for 1.5 h at 4 °C. Bound proteins were washed extensively and eluted with 250 mM imidazole in 20 mM Tris-HCl pH 7.5 and 150 mM NaCl. Proteins were further purified by size exclusion chromatography.

For Ub expression, purification protocols were adapted from previous studies⁷⁰. Harvested cells were resuspended in lysis buffer (20 mM ammonium acetate pH 5.1 and 0.1 mM PMSF), lysed by sonication, and clarified by centrifugation at 31,000 \times g for 30 min at 4 °C. The clarified lysate pH was lowered to 4.8 using glacial acetic acid and the solution was again centrifuged at 31,000 \times g for 30 min at 4 °C. The pH of the remaining soluble fraction was adjusted to 5.1 with the addition of NaOH. The supernatant was loaded onto a HiTrap SP cation exchange column equilibrated in 20 mM ammonium acetate pH 5.1. Ubiquitin was eluted with a buffer gradient to 0.5M ammonium acetate pH 5.1. Fractions corresponding to Ub were pooled and further

purified by size exclusion chromatography in 20 mM Tris pH 7.5, and 150 mM NaCl. Final fractions containing ubiquitin were collected and concentrated.

For Human E1 expression, purification protocols were adapted from previous studies⁶⁸. Briefly for 6xHis-Uba1, cells were harvested in lysis buffer (20 mM Tris pH 7.5, 150 mM NaCl, 1 mM PMSF, and cOmplete protease inhibitor) and lysed by sonication. After clarification, the supernatant was bound to cobalt resin, washed extensively, and eluted with 250 mM imidazole, 20 mM Tris pH 7.5, and 150 mM NaCl. Human E1 was further purified by reacting with ubiquitin conjugated to Affi-Gel 10. After incubation, the column was washed with 50 mM Tris-HCl pH 8.0 and 0.5 M KCl. Uba1 was eluted in 50 mM Tris-HCl pH 8.0 and 10 mM DTT, buffer exchanged to 50 mM Tris-HCl pH 8.0, 150 mM NaCl and further purified by size exclusion.

Synthesis of K63 Ub chains

Prior to synthesis, 5x PDBM buffer was prepared with the following components: 250 mM Tris-HCl pH 8.0, 25 mM MgCl₂, 50 mM creatine phosphate, 3 U/mL inorganic pyrophosphatase and 3 U/mL creatine phosphokinase. K63-linked poly-Ub was synthesized by incubating 0.1 μM human E1, 8 μM of Ubc13 and Mms2, 10 mg/mL WT-Ub, 5.6 mM ATP, 1x PDBM buffer, and 0.6 mM DTT. The reaction was incubated at 37 °C for 3 h and then the reaction was quenched by 20-fold dilution into 50 mM ammonium acetate, pH 4.5. The sample was loaded onto a HiTrap SP cation exchange column, and chains of defined lengths were separated using a linear gradient of 0–0.6 M NaCl. Peaks corresponding to di-Ub, tri-Ub, and tetra-Ub were pooled, and the buffer was exchanged into 20 mM Tris-HCl pH 7.5, 150 mM NaCl, and concentrated.

To generate K63 tri-Ub chains, we first generated three types of di-Ub chains: 1. Ub-R42K K63R and Ub-R42K D77; 2. Ub-R42K K63R and Ub-D77; 3. Ub-K63R and Ub-R42K D77. Following purification using a HiTrap SP cation exchange column, each di-Ub chain was treated with Yuh1 to remove the D77 at the proximal Ub⁶⁹. Tri-Ub chains were synthesized by reacting each di-Ub with either Ub-D77 or Ub-R42K D77. The sample was further purified by cation exchange, and buffer exchanged into 20 mM Tris-HCl pH 7.5, 150 mM NaCl.

In vitro synthesis of ubiquitinated Rab33B

To synthesize canonically ubiquitinated Rab33B, 4 μM of purified 4x-Flag-Rab33B was mixed with 50 mM Tris-HCl pH 8.0, 1x PDBM, 2.5 mM ATP, 0.15 μM human E1, 0.2 μM UbcH7, 0.5 μM SidC (aa. 1-542), and 100 μM ubiquitin. The reaction was incubated at 37 °C for 1.5 h. To synthesize mixed Ub chain-modified Rab33B, 4 μM 4x-Flag-Rab33B was incubated with 50 mM Tris-HCl pH 8.0, 1x PDBM, 2.5 mM ATP, 0.15 μM human E1, 0.2 μM UbcH7, 0.5 μM SidC (aa. 1-542), 1 μM SdeA-Core WT or SdeA-Core H227A mutant, 1 mM NAD⁺, and 100 μM ubiquitin at 37 °C for 2 h. In experiments using V5-tagged UbΔGG, Rab33B was first PR-ubiquitinated by SdeA and then ubiquitinated by SidC using WT-Ub as described above. Ubiquitinated Rab33B was then purified with anti-Flag beads for DUB cleavage or other assays.

In vitro UBA_{p62} binding assay

Purified GFP-UBA_{p62} was first immobilized to GFP-nanobody conjugated resins and incubated with in vitro ubiquitinated Rab33B at 4 °C for 2 h. The resin was washed with a buffer containing 50 mM Tris, pH 8.0 for 3 times and materials bound to the resin were analyzed by SDS-PAGE followed by Western blot using an anti-Ub antibody.

Poly-Ub chain modification assays

Ubiquitination reactions were performed by mixing 1 μM WT SdeA-Core or Sde-Core H277A mutant with 12.5 μM K63-linked tri-Ub or poly-Ub in a reaction buffer containing 50 mM Tris-HCl pH 7.5 and 50 mM NaCl, in the presence or absence of 1 mM NAD⁺. The reactions were incubated for 2 h at 37 °C and reaction products were assessed by 15%

SDS-PAGE stained with either Coomassie or Pro-Q Diamond phosphoprotein stain (Invitrogen). Only modified PR-Ub chains are visible by Pro-Q phosphoprotein stain due to its free phosphoryl group⁷¹.

DUB, DupA, and DupB cleavage assays

The cleavage reactions were performed by adding 1 μM of DUB, DupA, or DupB to in vitro synthesized poly-Ub chains or ubiquitinated substrates at 37 °C for 2 h. For poly-Ub chain cleavage, the reaction products were assessed by 15% SDS-PAGE stained with either Coomassie or Pro-Q Diamond phosphoprotein stain (Invitrogen). For the cleavage of ubiquitinated substrates, the supernatants of the cleavage reactions were first collected by centrifugation at 3300 × g. The supernatant was concentrated by precipitation with the addition of PPT (0.1% glacial acetic acid, 49.9% ethanol, and 50% acetone) for 1 h on ice. The protein pellets were resuspended in SDS loading buffer. The resins were washed 3 times with 50 mM Tris pH 8.0 and the remaining proteins attached to the resin were eluted with 1% SDS and 100 mM Tris pH 8.0. Samples were separated by 15% SDS-PAGE followed by Western blot using an anti-Ub antibody or stained with Pro-Q Diamond phosphoprotein stain.

Cell culture and transfection

HEK293T and U937 cells were cultured at 37 °C with 5% CO₂, in Dulbecco's modified Eagle's medium (Corning) and RPMI 1640 medium (Corning) respectively, both medium were supplemented with 10% fetal bovine serum (Gibco) and 1% penicillin-streptomycin (Invitrogen). Transfection was performed using a polyethyleneimine (PEI) reagent.

Legionella strains and infection

L. pneumophila strains used include the wild type Lp02⁷², the Dot/Icm deficient Lp03⁷², the Δ*sde* strain⁷³, the Δ*sdc* strain²⁴, and the Δ*sde/sdc* strain, which was created in this study. Complementation strains were generated by electroporation of pZL507 plasmids containing wild-type or mutant SdeA or SidC.

For *Legionella* infections, HEK293T cells were transfected with FCyRII and HA-Ub, EGFP-Rab1, 3xFlag-Rab1, 4xFlag-Rab33B or LULL1-HA for 24 h. For U937 cell infection, cells differentiation was induced with 10 ng/mL phorbol 12-myristate 13-acetate (PMA) for 2 days before infection. Bacteria of indicated *Legionella* strains were opsonized with rabbit anti-*L. pneumophila* antibodies (1:500) at 37 °C for 20 min before infection. The HEK293T cells were infected with post-exponential *L. pneumophila* strains at an MOI of 2 (for confocal imaging), or 20 (for Western blot) for the indicated amount of time.

Immunoprecipitation and Western blot

For the enrichment of in vivo ubiquitinated substrates, Rab1, Rab33B, LULL1, or Stx17, transfected HEK293T cells were challenged with the Lp strains for the indicated amount of times and then the cells were lysed in ice-cold RIPA buffer (50 mM Tris pH 7.5, 150 mM NaCl, 1% Triton, 0.1% SDS, 0.5% deoxycholic acid) with protease inhibitor cocktail (Roche). Samples were sonicated and then centrifuged at 18,000 × g for 20 min at 4 °C. The supernatant was incubated with 50% slurry of the EZview Red Anti-Flag M2 Affinity Gel Beads (Sigma, F2426), EZview Red Anti-HA Affinity Gel beads (Sigma, E6779) or GFP-nanobody conjugated resins for 2 h for immunoprecipitation of 3xFlag-Rab1, 4xFlag-Rab33B, Flag-Stx17, HA-Rab33B, LULL1-HA, or EGFP-3xFlag-Rab1.

For co-immunoprecipitation, FCyRII, 3xFlag-Rab1, and HA-p62 transfected HEK293T cells were infected with specified Lp strains for 1 h. Cells were then lysed in ice-cold lysis buffer (50 mM Tris pH 7.5, 150 mM NaCl, 1% Triton, 0.5% deoxycholic acid, 5 mM EDTA, 5% glycerol) with protease inhibitor cocktail (Roche) for 30 min. 5% of the supernatant was used as input and the rest was mixed with anti-Flag beads for 2 h for immunoprecipitation of 3xFlag-Rab1.

All Western blots were performed according to standard procedure. Briefly, samples were boiled and separated by gel electrophoresis

with 12% or 15% SDS-PAGE gels and transferred to a PVDF (GE HealthCare) or nitrocellulose (MilliporeSigma) membrane. Membranes were incubated for 1 h in 5% milk (Carnation) in TBST. Milk was washed and membranes were incubated overnight with indicated primary antibodies. Secondary antibodies used were Alexa Fluor donkey anti-mouse 680 (Invitrogen) or donkey anti-rabbit RDye 800CW (LI-COR) at 1:10,000 dilutions. Membranes were scanned using the LI-COR Odyssey CLx Imager and processed using ImageStudio Lite software (v.5.2).

Antibodies, immunostaining, and fluorescent microscopy

Anti-HA (Sigma-Aldrich), anti-Flag (Proteintech), anti-V5 (Bio-Rad), anti-Calnexin (Invitrogen), and anti-Ub (BioLegend) antibodies were purchased commercially. Anti-*L. pneumophila* antibodies were previously generated⁴⁴. *Legionella* bacterium staining was performed following procedures established in previous studies⁴⁴. Infected HEK293T cells expressing FCyRII and HA-Ub, EGFP-Rab1, LULL1-HA, EGFP-sec61 β , or mCherry-p62 were fixed using 4% PFA. Extracellular bacteria were incubated with rabbit anti-*L. pneumophila* primary antibody and then with Alexa Fluor donkey anti-rabbit 647 nm secondary antibody. The cells were then permeabilized with 0.1% triton and incubated with rabbit anti-*L. pneumophila* primary antibody, and then stained with Alexa Fluor donkey anti-rabbit 568 nm or 488 nm secondary antibody. HA-Ub or LULL1-HA was stained using a mouse anti-HA primary antibody and donkey anti-mouse 488 nm secondary antibody. Calnexin was stained using a rabbit anti-Calnexin primary antibody and donkey anti-mouse 488 nm secondary antibody.

Images were captured on a spinning disk confocal microscope (Intelligent Imaging Innovations, Denver, CO) with a spinning disk confocal unit (Yokogawa CSU-X1), a fiber-optic laser light source, an inverted microscope (Leica DMI6000B), a 100 \times 1.47 NA objective lens, and a Hamamatsu ORCA Flash 4.0 v2+ sCMOS camera. Images were captured using SlideBook 6.0 software and analyzed using ImageJ software v.1.53 (NIH).

Mass spectrometry sample preparation

Ubiquitinated EGFP-3xFlag-Rab1 or 4xFlag-Rab33B from wild-type Lp strain infected HEK293T cells were purified using anti-GFP-nanobody conjugated beads or Flag-beads, respectively. 4xFlag-Rab33B in vitro ubiquitination reactions were performed as described above. For elution samples, EGFP-3x-Flag-Rab1 or 4x-Flag-Rab33B was eluted by incubating the resin (GFP-nanobeads or Flag-beads) with elution buffer containing 1% SDS in 100 mM Tris pH 8.0 at 65 °C for 15 min. For DUB cleavage samples, ubiquitinated samples were treated with 1 μ M of SdeA DUB as described above to yield predominantly mono-Ub species. Eluted or DUB-treated samples were reduced with 10 mM DTT and alkylated with 25 mM iodoacetamide. Samples were then precipitated in PPT (0.1% glacial acetic acid, 49.9% ethanol, and 50% acetone) on ice for 1 h. Proteins were pelleted and resolubilized in 8 M Urea in 50 mM Tris pH 8.0. Samples were then digested with Pierce trypsin protease MS-grade (Thermo Scientific) at 37 °C overnight. Trypsinized samples were acidified with the addition of trifluoroacetic acid and formic acid, bound to a C18 column (Waters), and washed with 0.1% acetic acid. Peptides were eluted in 80% acetonitrile and 0.1% acetic acid and dried in a speed-vac. Samples were resuspended in 0.1 picomol/ μ L of angiotensin in 0.1% trifluoroacetic acid.

Mass spectrometry and data analysis

Peptides were analyzed using an EASY-nLC 1200 System (catalog no. LC140; Thermo Scientific) equipped with an in-house 3 μ m C18 resin (Michrom BioResources) packed capillary column (125 μ m \times 30 cm) coupled to an Orbitrap Fusion Lumos Tribrid Mass Spectrometer (catalog no. IQLAAEGAAPFADBMBHQ; Thermo Scientific). MS1 precursors were detected at m/z = 375–1500 and resolution = 240,000. The AGC target and maximum injection time were set at STANDARD and 50 ms. Precursor ions with a charge of 2+ to 7+ were isolated with an isolation

window of 1.2 for MS2 analysis. Here, ions were isolated in the quadrupole and collected to standard AGC target and fragmented by high energy dissociation with a collision energy of 32%. Spectra were recorded using Thermo Xcalibur Software v.4.4 (catalog no. OPTON-30965; Thermo Scientific) and Tune application v.3.0 (Thermo Scientific).

Raw files were searched using Proteome Discoverer Software 2.3 (Thermo Scientific). The protein sequence database was the UniProt human database. The peptide identification and quantification pipeline relied on tools from the trans-proteomic pipeline (TPP). PhosphoRibose of arginine (+212.009 Da), and GG motif of lysine (+114.043 Da). Cysteine carbamidomethyl (+57.021 Da) was set as a static modification. Search parameters specified precursor mass and fragment mass tolerance of 15 ppm. Spectra were searched with the SEQUEST HT or Comet (v. 2019.01.1) search engine and validated with Percolator or PeptideProphet algorithm. All results were filtered using the following parameters: the minimum probability of 0.9, minimum peptide length of 7 amino acid residues, accurate mass binning, and restriction to +2, +3, and +4 ion charge states. Phosphoribosylated peptides were then evaluated by PTMProphet to obtain a localization score for the modification⁷⁴.

Reporting summary

Further information on research design is available in the Nature Portfolio Reporting Summary linked to this article.

Data availability

The mass spectrometry proteomics data has been deposited to the ProteomeXchange Consortium via the PRIDE partner repository with the dataset identifier [PXD045494](https://doi.org/10.26434/chemrxiv-2024-pxd04) and [PXD046135](https://doi.org/10.26434/chemrxiv-2024-pxd04). Source data are provided with this paper.

References

1. Cuervo, A. M. Autophagy: in sickness and in health. *Trends Cell Biol.* **14**, 70–77 (2004).
2. Shintani, T. & Klionsky, D. J. Autophagy in health and disease: a double-edged sword. *Science* **306**, 990–995 (2004).
3. Yang, Z. & Klionsky, D. J. Mammalian autophagy: core molecular machinery and signaling regulation. *Curr. Opin. Cell Biol.* **22**, 124–131 (2010).
4. Lin, M. G. & Hurlley, J. H. Structure and function of the ULK1 complex in autophagy. *Curr. Opin. Cell Biol.* **39**, 61–68 (2016).
5. Nakatogawa, H., Ichimura, Y. & Ohsumi, Y. Atg8, a ubiquitin-like protein required for autophagosome formation, mediates membrane tethering and hemifusion. *Cell* **130**, 165–178 (2007).
6. Ohsumi, Y. Molecular dissection of autophagy: two ubiquitin-like systems. *Nat. Rev. Mol. Cell Biol.* **2**, 211–216 (2001).
7. Mizushima, N. Autophagy: process and function. *Genes Dev.* **21**, 2861–2873 (2007).
8. Vargas, J. N. S., Hamasaki, M., Kawabata, T., Youle, R. J. & Yoshimori, T. The mechanisms and roles of selective autophagy in mammals. *Nat. Rev. Mol. Cell Biol.* **24**, 167–185 (2023).
9. Kirkin, V. & Rogov, V. V. A diversity of selective autophagy receptors determines the specificity of the autophagy pathway. *Mol. Cell* **76**, 268–285 (2019).
10. Mostowy, S. et al. p62 and NDP52 proteins target intracytosolic *Shigella* and *Listeria* to different autophagy pathways. *J. Biol. Chem.* **286**, 26987–26995 (2011).
11. von Muhlinen, N., Thurston, T., Ryzhakov, G., Bloor, S. & Randow, F. NDP52, a novel autophagy receptor for ubiquitin-decorated cytosolic bacteria. *Autophagy* **6**, 288–289 (2010).
12. Fraser, D. W. et al. Legionnaires' disease: description of an epidemic of pneumonia. *N. Engl. J. Med.* **297**, 1189–1197 (1977).
13. McDade, J. E. et al. Legionnaires' disease: isolation of a bacterium and demonstration of its role in other respiratory disease. *N. Engl. J. Med.* **297**, 1197–1203 (1977).

14. Burstein, D. et al. Genomic analysis of 38 *Legionella* species identifies large and diverse effector repertoires. *Nat. Genet* **48**, 167–175 (2016).
15. Gomez-Valero, L. et al. More than 18,000 effectors in the *Legionella* genus genome provide multiple, independent combinations for replication in human cells. *Proc. Natl Acad. Sci. USA* **116**, 2265–2273 (2019).
16. Isberg, R. R., O'Connor, T. J. & Heidtman, M. The *Legionella pneumophila* replication vacuole: making a cosy niche inside host cells. *Nat. Rev. Microbiol* **7**, 13–24 (2009).
17. Hershko, A. & Ciechanover, A. The ubiquitin system. *Annu Rev. Biochem.* **67**, 425–479 (1998).
18. Chen, Z. J. & Sun, L. J. Nonproteolytic functions of ubiquitin in cell signaling. *Mol. Cell* **33**, 275–286 (2009).
19. Hurlley, J. H. & Stenmark, H. Molecular mechanisms of ubiquitin-dependent membrane traffic. *Annu. Rev. Biophys.* **40**, 119–142 (2011).
20. Haglund, K. & Dikic, I. The role of ubiquitylation in receptor endocytosis and endosomal sorting. *J. Cell Sci.* **125**, 265–275 (2012).
21. Dorer, M. S., Kirton, D., Bader, J. S. & Isberg, R. R. RNA interference analysis of *Legionella* in *Drosophila* cells: exploitation of early secretory apparatus dynamics. *PLoS Pathog.* **2**, e34 (2006).
22. Ivanov, S. S. & Roy, C. R. Modulation of ubiquitin dynamics and suppression of DALIS formation by the *Legionella pneumophila* Dot/Icm system. *Cell Microbiol.* **11**, 261–278 (2009).
23. Horenkamp, F. A. et al. *Legionella pneumophila* subversion of host vesicular transport by SidC effector proteins. *Traffic* **15**, 488–499 (2014).
24. Hsu, F. et al. The *Legionella* effector SidC defines a unique family of ubiquitin ligases important for bacterial phagosomal remodeling. *Proc. Natl Acad. Sci. USA* **111**, 10538–10543 (2014).
25. Sheedlo, M. J. et al. Structural basis of substrate recognition by a bacterial deubiquitinase important for dynamics of phagosome ubiquitination. *Proc. Natl Acad. Sci. USA* **112**, 15090–15095 (2015).
26. Qiu, J. et al. Ubiquitination independent of E1 and E2 enzymes by bacterial effectors. *Nature* **533**, 120–124 (2016).
27. Bhogaraju, S. et al. Phosphoribosylation of ubiquitin promotes serine ubiquitination and impairs conventional ubiquitination. *Cell* **167**, 1636–1649.e1613 (2016).
28. Kotewicz, K. M. et al. A single *Legionella* effector catalyzes a multistep ubiquitination pathway to rearrange tubular endoplasmic reticulum for replication. *Cell Host Microbe* **21**, 169–181 (2017).
29. Akturk, A. et al. Mechanism of phosphoribosyl-ubiquitination mediated by a single *Legionella* effector. *Nature* **557**, 729–733 (2018).
30. Dong, Y. et al. Structural basis of ubiquitin modification by the *Legionella* effector SdeA. *Nature* **557**, 674–678 (2018).
31. Kalayil, S. et al. Insights into catalysis and function of phosphoribosyl-linked serine ubiquitination. *Nature* **557**, 734–738 (2018).
32. Wang, Y. et al. Structural insights into non-canonical ubiquitination catalyzed by SidE. *Cell* **173**, 1231–1243.e1216 (2018).
33. Kim, L. et al. Structural and biochemical study of the mono-ADP-ribosyltransferase domain of sdea, a ubiquitylating/deubiquitylating enzyme from *Legionella pneumophila*. *J. Mol. Biol.* **430**, 2843–2856 (2018).
34. Zhang, M. et al. Members of the *Legionella pneumophila* Sde family target tyrosine residues for phosphoribosyl-linked ubiquitination. *RSC Chem. Biol.* **2**, 1509–1519 (2021).
35. Sulpizio, A. G., Minelli, M. E. & Mao, Y. Glutamylation of bacterial ubiquitin ligases by a legionella pseudokinase. *Trends Microbiol* **27**, 967–969 (2019).
36. Omotade, T. O. & Roy, C. R. *Legionella pneumophila* excludes autophagy adaptors from the ubiquitin-labeled vacuole in which it resides. *Infect. Immun.* **88**, e00793–19 (2020).
37. Choy, A. et al. The *Legionella* effector RavZ inhibits host autophagy through irreversible Atg8 deconjugation. *Science* **338**, 1072–1076 (2012).
38. Rolando, M. et al. *Legionella pneumophila* S1P-lyase targets host sphingolipid metabolism and restrains autophagy. *Proc. Natl Acad. Sci. USA* **113**, 1901–1906 (2016).
39. Rolando, M., Escoll, P. & Buchrieser, C. *Legionella pneumophila* restrains autophagy by modulating the host's sphingolipid metabolism. *Autophagy* **12**, 1053–1054 (2016).
40. Arasaki, K. & Tagaya, M. *Legionella* blocks autophagy by cleaving STX17 (syntaxin 17). *Autophagy* **13**, 2008–2009 (2017).
41. Murata, M. et al. Requirement of phosphatidic acid binding for distribution of the bacterial protein Lpg1137 targeting syntaxin 17. *J. Cell Sci.* **135**, jcs259538 (2022).
42. Jeng, E. E. et al. Systematic identification of host cell regulators of *Legionella pneumophila* pathogenesis using a genome-wide CRISPR screen. *Cell Host Microbe* **26**, 551–563.e556 (2019).
43. Shin, D. et al. Regulation of phosphoribosyl-linked serine ubiquitination by deubiquitinases DupA and DupB. *Mol. Cell* **77**, 164–179.e166 (2020).
44. Wan, M. et al. Deubiquitination of phosphoribosyl-ubiquitin conjugates by phosphodiesterase-domain-containing *Legionella* effectors. *Proc. Natl Acad. Sci. USA* **116**, 23518–23526 (2019).
45. Swanson, K. A., Hicke, L. & Radhakrishnan, I. Structural basis for monoubiquitin recognition by the Ede1 UBA domain. *J. Mol. Biol.* **358**, 713–724 (2006).
46. Daniels, C. M., Ong, S. E. & Leung, A. K. Phosphoproteomic approach to characterize protein mono- and poly(ADP-ribosylation) sites from cells. *J. Proteome Res.* **13**, 3510–3522 (2014).
47. Ge, J. et al. Phosphoribosyl-linked serine ubiquitination of USP14 by the SidE family effectors of *Legionella* excludes p62 from the bacterial phagosome. *Cell Rep.* **42**, 112817 (2023).
48. Kirkin, V., McEwan, D. G., Novak, I. & Dikic, I. A role for ubiquitin in selective autophagy. *Mol. Cell* **34**, 259–269 (2009).
49. Kotewicz, K. M. et al. Sde proteins coordinate ubiquitin utilization and phosphoribosylation to establish and maintain the *Legionella* replication vacuole. *Nat. Commun.* <https://doi.org/10.1038/s41467-024-51272-2> (2023).
50. Swanson, M. S. & Isberg, R. R. Association of *Legionella pneumophila* with the macrophage endoplasmic reticulum. *Infect. Immun.* **63**, 3609–3620 (1995).
51. Tilney, L. G., Harb, O. S., Connelly, P. S., Robinson, C. G. & Roy, C. R. How the parasitic bacterium *Legionella pneumophila* modifies its phagosome and transforms it into rough ER: implications for conversion of plasma membrane to the ER membrane. *J. Cell Sci.* **114**, 4637–4650 (2001).
52. Kagan, J. C. & Roy, C. R. *Legionella* phagosomes intercept vesicular traffic from endoplasmic reticulum exit sites. *Nat. Cell Biol.* **4**, 945–954 (2002).
53. Kawabata, M. et al. *Legionella* hijacks the host Golgi-to-ER retrograde pathway for the association of *Legionella*-containing vacuole with the ER. *PLoS Pathog.* **17**, e1009437 (2021).
54. Lin, Y. H. & Machner, M. P. Exploitation of the host cell ubiquitin machinery by microbial effector proteins. *J. Cell Sci.* **130**, 1985–1996 (2017).
55. Qiu, J. & Luo, Z. Q. Hijacking of the host ubiquitin network by *Legionella pneumophila*. *Front. Cell Infect. Microbiol* **7**, 487 (2017).
56. Price, C. T. D. & Abu Kwaiq, Y. Evolution and adaptation of *Legionella pneumophila* to manipulate the ubiquitination machinery of its amoebae and mammalian hosts. *Biomolecules* **11**, 112 (2021).

57. Tomaskovic, I., Gonzalez, A. & Dikic, I. Ubiquitin and *Legionella*: from bench to bedside. *Semin Cell Dev. Biol.* **132**, 230–241 (2022).
58. Lin, Y. H. et al. RavN is a member of a previously unrecognized group of *Legionella pneumophila* E3 ubiquitin ligases. *PLoS Pathog.* **14**, e1006897 (2018).
59. Ma, K. et al. The bacterial deubiquitinase Ceg23 regulates the association of Lys-63-linked polyubiquitin molecules on the *Legionella* phagosome. *J. Biol. Chem.* **295**, 1646–1657 (2020).
60. Shin, D. et al. Bacterial OTU deubiquitinases regulate substrate ubiquitination upon *Legionella* infection. *Elife* **9**, e58277 (2020).
61. Kubori, T., Kitao, T., Ando, H. & Nagai, H. LotA, a *Legionella* deubiquitinase, has dual catalytic activity and contributes to intracellular growth. *Cell Microbiol.* **20**, e12840 (2018).
62. Liu, S. et al. Interplay between bacterial deubiquitinase and ubiquitin E3 ligase regulates ubiquitin dynamics on *Legionella phagosomes*. *Elife* **9**, e58114 (2020).
63. Wan, M. et al. A bacterial effector deubiquitinase specifically hydrolyses linear ubiquitin chains to inhibit host inflammatory signalling. *Nat. Microbiol.* **4**, 1282–1293 (2019).
64. Urbanus, M. L. et al. Diverse mechanisms of metaeffector activity in an intracellular bacterial pathogen, *Legionella pneumophila*. *Mol. Syst. Biol.* **12**, 893 (2016).
65. Price, C. T. et al. Molecular mimicry by an F-box effector of *Legionella pneumophila* hijacks a conserved polyubiquitination machinery within macrophages and protozoa. *PLoS Pathog.* **5**, e1000704 (2009).
66. Price, C. T., Al-Quadan, T., Santic, M., Rosenshine, I. & Abu Kwaik, Y. Host proteasomal degradation generates amino acids essential for intracellular bacterial growth. *Science* **334**, 1553–1557 (2011).
67. Lomma, M. et al. The *Legionella pneumophila* F-box protein Lpp2082 (AnkB) modulates ubiquitination of the host protein parvin B and promotes intracellular replication. *Cell Microbiol.* **12**, 1272–1291 (2010).
68. Wasilko, D. J., Huang, Q. & Mao, Y. Insights into the ubiquitin transfer cascade catalyzed by the *Legionella* effector SidC. *Elife* **7**, e36154 (2018).
69. Zhu, L. et al. Adaptor linked K63 di-ubiquitin activates Nedd4/Rsp5 E3 ligase. *Elife* **11**, e77424 (2022).
70. Raasi, S. & Pickart, C. M. Ubiquitin chain synthesis. *Methods Mol. Biol.* **301**, 47–55 (2005).
71. Steinberg, T. H. et al. Global quantitative phosphoprotein analysis using Multiplexed Proteomics technology. *Proteomics* **3**, 1128–1144 (2003).
72. Berger, K. H. & Isberg, R. R. Two distinct defects in intracellular growth complemented by a single genetic locus in *Legionella pneumophila*. *Mol. Microbiol.* **7**, 7–19 (1993).
73. Jeong, K. C., Sexton, J. A. & Vogel, J. P. Spatiotemporal regulation of a *Legionella pneumophila* T4SS substrate by the metaeffector SidJ. *PLoS Pathog.* **11**, e1004695 (2015).
74. Shteynberg, D. D. et al. PTMPProphet: fast and accurate mass modification localization for the trans-proteomic pipeline. *J. Proteome Res.* **18**, 4262–4272 (2019).

Acknowledgements

We thank Dr. Zhaoqing-Luo (Purdue Univ.) for providing plasmids (FcyR1I, pCMV-4xFlag-Rab33B). We also thank Dr. Joseph Vogel (Wash. Univ.) for the Δ sde strain and Dr. Fenghua Hu (Cornell Univ.) for the plasmids (mCherry-p62 and HA-p62). This work was supported by the National Institutes of Health (NIH) Grants R01-GM135379-01 (Y.M.), R01-HD095296 (M.B.S.), R35-GM141159 (M.B.S.), and RM1-GM139738 (H.Y.).

Author contributions

M.W., M.E.M., and Y.M. conceived the project. M.W., M.E.M., Q.Z., and S.M. performed the experiments. M.W., M.E.M., Q.Z., S.M., H.Y., M.B.S., and Y.M. analyzed the data. M.W., M.E.M., and Y.M. wrote the paper.

Competing interests

The authors declare no competing interests.

Additional information

Supplementary information The online version contains supplementary material available at <https://doi.org/10.1038/s41467-024-51273-1>.

Correspondence and requests for materials should be addressed to Yuxin Mao.

Peer review information *Nature Communications* thanks Yousef Abu Kwaik, and the other, anonymous, reviewer(s) for their contribution to the peer review of this work. A peer review file is available.

Reprints and permissions information is available at <http://www.nature.com/reprints>

Publisher's note Springer Nature remains neutral with regard to jurisdictional claims in published maps and institutional affiliations.

Open Access This article is licensed under a Creative Commons Attribution-NonCommercial-NoDerivatives 4.0 International License, which permits any non-commercial use, sharing, distribution and reproduction in any medium or format, as long as you give appropriate credit to the original author(s) and the source, provide a link to the Creative Commons licence, and indicate if you modified the licensed material. You do not have permission under this licence to share adapted material derived from this article or parts of it. The images or other third party material in this article are included in the article's Creative Commons licence, unless indicated otherwise in a credit line to the material. If material is not included in the article's Creative Commons licence and your intended use is not permitted by statutory regulation or exceeds the permitted use, you will need to obtain permission directly from the copyright holder. To view a copy of this licence, visit <http://creativecommons.org/licenses/by-nc-nd/4.0/>.

© The Author(s) 2024